International Journal of Earth Sciences (2019) 108:887–910
https://doi.org/10.1007/s00531-019-01683-0

ORIGINAL PAPER

U–Pb ages of magmatic and detrital zircon of the Döhlen Basin: geological history of a Permian strike-slip basin in the Elbe Zone (Germany)

J. Zieger[1] · L. Bittner[2,3] · A. Gärtner[1] · M. Hofmann[1] · A. Gerdes[4] · L. Marko[4] · U. Linnemann[1]

Received: 19 July 2018 / Accepted: 30 January 2019 / Published online: 12 February 2019

Abstract

The post-orogenic evolution of Variscan Central Europe is characterized by the formation of numerous basins. The early Permian Döhlen Basin is located in the Elbe Zone (Germany) and is bordered by metamorphic rocks of the Erzgebirge and numerous Variscan magmatic complexes. The NW–SE-oriented basin is evidence for a major rearrangement of stress fields during the post-Variscan reactivation of fault zones in Central Europe. Eleven samples of magmatic rocks and sediments have been analyzed with respect to their U–Th–Pb isotope ratios and geochemical composition. Of three magmatic samples (two tuffs, one trachyandesite), we analyzed 170 zircon grains. The Unkersdorf Tuff of the Unkersdorf Formation gave an age of 294 ± 3 Ma (Upper Asselian to Sakmarian), whereas a trachyandesite of the same formation was dated at 293 ± 5 Ma (Lower Artinskian to Lower Asselian). The Wachtelberg Ignimbrite (Upper Bannewitz Formation) showed an age of 286 ± 4 Ma (Artinskian to Lower Kungurian). As the first study, we also analyzed 984 detrital zircon grains of nine Late Paleozoic Central European sandstone and conglomerate samples of the Niederhäslich Formation and the Bannewitz Formation with respect to their U–Pb age composition. All sediments but two yielded two distinct age groups between 295 and 340 Ma and 530–750 Ma, as well as a minor amount of Precambrian zircon ages. Geochemical data points to an active margin setting with developing strike-slip basins. The data suggests a c. 10 Ma lasting basin formation during the second culmination of volcano-tectonic activity with basic to intermediate melts. The second youngest formation (Niederhäslich Formation) consists predominantly of pre-Permian basement material, which implies only minor volcanic activity and erosion from adjacent basement blocks. On the contrary, the uppermost and youngest Bannewitz Formation features strong evidence for volcanic activity in the neighboring area of the basin. The present study strongly suggests a rapid basin development and further shows how the evolution of the Döhlen Basin is proof for several post-Variscan tectonic reactivation phases in Sakmarian and Lower Kungurian of Central Europe. Finally, our results exemplarily show how basin evolution may be characterized by radiometric data of detrital zircon grains.

Keywords Döhlen Basin · U–Pb–Th geochronology · Zircon · Pyroclastic rocks · Variscides

Electronic supplementary material The online version of this article (https://doi.org/10.1007/s00531-019-01683-0) contains supplementary material, which is available to authorized users.

✉ J. Zieger
Johannes.Zieger@senckenberg.de

[1] Museum of Mineralogy and Geology, Department of Geochronology, Senckenberg Natural History Collections Dresden, Koenigsbruecker Landstr. 159, 01109 Dresden, Germany

[2] Faculty of Environmental Sciences, Department of Geography, Technical University Dresden, Helmholzstr. 10, 01069 Dresden, Germany

[3] Institute of Agronomy and Nutritional Sciences, Soil Biogeochemistry, Martin-Luther University Halle-Wittenberg, Von-Seckendorff-Platz 3, 06120 Halle (Saale), Germany

[4] Department of Geoscience, Mineralogy, Goethe University Frankfurt, Altenhoeferallee 1, 60438 Frankfurt, Germany

Introduction

The Döhlen Basin is famous for the earliest Permian plants, which are preserved in situ by volcanic ash falls (Rößler and Barthel 1998). The fossils were discovered in the course of intensive coal mining which lasted several hundred years.

The formation of the Döhlen Basin is strongly associated with the supercontinent Pangea. The formation of this supercontinent is associated with several Paleozoic orogenic processes across Europe. One of them is the Variscan orogeny, which is interpreted as a result of the closure of the Rheic Ocean, which separated Gondwana from Laurussia. Aligned along the Rheic suture, several Cadomian and Variscan massifs provide insight into the composition of different terranes and cratons involved into the Variscan Orogeny. For Central Europe, e.g., the Armorican Massif, the French Massif Central and the Bohemian Massif are important. The latter comprises mainly areas of eastern Germany and the Czech Republic (Fig. 1), and is subdivided into the Saxo-Thuringian Zone, the Teplá Barrandian Unit, the Moldanubian Zone, the Sudetes and the Moraves Silesian Zone. A more detailed description of the evolution of the Rheic Ocean and the geology of the Saxo-Thuringian Zone can be found in, e.g., Franke (2000), Franke and Żelaźniewicz (2002), Linnemann (2003a, b), Kroner et al. (2007), Linnemann et al. (2008a) and Nance et al. (2008).

The molasses of these orogens led to the formation of a variety of Permian basins. This debris represents a record of the tectonic and magmatic activity of the Variscan orogeny.

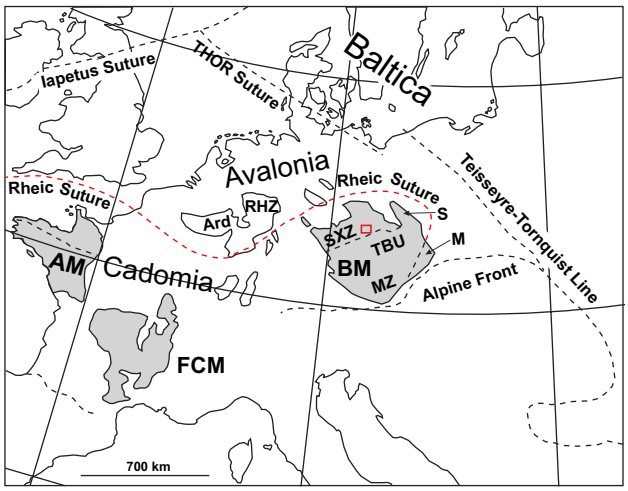

Fig. 1 Cadomian and Variscan Massifs in Southwestern and Central Europe with Variscan oceanic suture of the Rheic Ocean (red line; modified after Robardet 2002; Linnemann et al. 2007, 2008a). *AM* Armorican Massif, *FMC* French Massif Central, *BM* Bohemian Massif, *SXZ* Saxo-Thuringian Zone, *TBU* Teplá-Barrandian Unit, *MZ* Moldanubian Zone, *S* Sudetes, *M* Moravo-Silesian Zone, *RHZ* Rheno-Hercynian Zone, *Ard* Ardennes

One of these basins is the Döhlen Basin, which is located SW of Dresden (Saxony) between the Elbe valley and the Erzgebirge. Volcano-tectonic events intensively affected the basin, because it is located in the area of the Elbe lineament (Pietzsch 1956; Stille 1949; Tröger et al. 1968). The maximum fill of about 700–800 m can be subdivided into four fining up megacycles (formations), which are confined by an abundance of volcanic and volcanoclastic rocks. In contrast to other Permo-Carboniferous basins, up to 50% of the basin fill is comprised of pyroclastic rocks (Schneider and Hoffman 2001). In close proximity of the basin, there are several late Paleozoic volcanic complexes, like the caldera of the Tharandter Wald and the Meissen Volcanic Complex as well as the Paleozoic Nossen-Wilsdruff and Elbe Valley Slate Complexes.

Here we present the first detrital U–Pb and $_{\varepsilon}$HF(t) zircon study on Late Paleozoic sediments of Central Europe, which enables us to give a coherent model about timing and sediment fluxes during the evolution of the Döhlen Basin. It also gives new insights into the origin of late post-Variscan magmas.

Evolution of the Rheic Ocean and a brief geological history of the Saxo-Thuringian Zone

The Elbe Zone is part of the Saxo-Thuringian Zone, which is situated in the north of the Bohemian Massif (Kossmat 1927; Fig. 1) and features evidence of Cadomian and Variscan orogenic processes. The oldest preserved rocks of the Elbe Zone are c. 580–560 Ma old turbiditic greywackes (Linnemann et al. 2008b). The Neoproterozoic sediments are thought to have been deposited in a back-arc and retro-arc basin setting along the northern active margin of Gondwana during the Cadomian Orogeny (Linnemann et al. 2007). These units were deformed by an arc-continent collision and were intruded by voluminous granitoid bodies at c. 540 Ma (e.g. Gehmlich 2003; Tichomirowa et al. 2001; Linnemann et al. 2007). Linnemann et al. (2007) interpreted this high magmatic activity as a reaction to a slab break off caused by the subduction of a heavier oceanic plate. Due to a general change of the geological situation from an arc to a transform margin comparable to the present-day Basin and Range Province in Western USA, the opening of the Rheic Ocean was possible (e.g., Pin and Marini 1993; Nance and Murphy 1996; Kryza and Pin 1997; Nance et al. 2002).

The opening of the Rheic Ocean in Upper Cambrian (c. 500–485 Ma) was accompanied by an upwelling asthenosphere, which led to a thinning of northern peri-Gondwanan crust and an increased magmatic activity (e.g., Borkowska et al. 1980; Kröner et al. 1994; Gehmlich et al. 1997; Linnemann et al. 2007; Pin et al. 2007; Oberc-Dziedzic et al.

2009; Białek et al. 2014). After the complete opening of the Rheic Ocean at c. 480 Ma, the following Lower Ordovician to mid Devonian is characterized by a tectonic and magmatic quiescence with shelf sedimentation. The Ordovician shelf sediments of the Frauenbach and Phycodes groups in the Schwarzburg Anticline of the Saxo-Thuringian Zone reach a thickness up to 3000 m (Linnemann and Romer 2002) and are interpreted as deposits of the passive margin of northern Gondwana (Linnemann et al. 2007).

The closure of the Rheic Ocean began in the Lower Devonian with the continuing northward drift of Gondwana towards Laurussia (Romer et al. 2003, Nance et al. 2012). With the Upper Devonian collision of Gondwana with Laurussia c. 370–360 Ma, the initial closing of the Rheic Ocean began (Kroner et al. 2007) and the result was crustal stacking, while subduction of Gondwanan Cadomic crust continued (Kroner et al. 2007, 2010). Ongoing Variscan Orogeny in Central Europe in the Lower Carboniferous times (360–340 Ma) caused transpression, HP/LT metamorphism and plutonism (Kroner et al. 2007; Sagawe et al. 2016). These high-pressure metamorphic units (allochthonous domains) are associated with Neoproterozoic and Paleozoic low-grade metamorphic successions (autochthonous domains, Kroner et al. 2007). Due to different crustal thicknesses during the collision of Gondwana with Laurussia, thinned peri-Gondwanan and possible peri-Baltic or Avalonian crust was subducted (Saxonian Granulite Massif, parts of the Erzgebirge), whereas rigid crustal parts like the Lausitz Block remained stable (Kroner et al. 2007; Sagawe et al. 2016).

Today the allochthonous domains are surrounded by a wrench and thrust zone termed the Elbe Zone, which is part of the much larger Cretaceous—early Cenozoic Elbe Fault System (e.g., Bayer et al. 2002; Knape 1963a, b; Tröger et al. 1968). This compressional event affected large parts of Central Europe and was caused by the opening of the Northern Atlantic Ocean and Alpine convergence (Ziegler 1990). In Late Paleozoic, the Elbe Zone was part of a major post-Variscan wrench fault caused by dextral translation of the Armorican-European and African plate (Arthaud and Matte 1977). The Elbe Zone as the southeastern end of this fault system is interpreted as a dextral strike-slip zone between the Erzgebirge and the Lausitz Block (Kroner et al. 2007; Mattern 1996; Linnemann 1994; Linnemann and Schauer 1999). Mattern (1996) estimated the Late Paleozoic displacement of 60–120 km, whereas Katzung (1995) calculated a displacement of 10–15 km of the transtensional movement between the now separated autochthonous Lausitz Block and allochthonous Erzgebirge.

During the late phase of the Variscan Orogeny in the Late Paleozoic (c. 340–295 Ma), an increased magmatism and reactivation of existing faults took place in Central Europe (Hofmann et al. 2009; Förster and Romer 2010; Hoffmann et al. 2013; and references therein). A first peak of high-grade metamorphism occurred in the Pennsylvanian due to transtensional tectonics (Ahrendt et al. 1983). Because of major strike-slip movements at the Carboniferous/Permian transition, a second extended period of volcanic and subvolcanic silica-rich activity took place (e.g., Arthaud and Matte 1977; Lorenz and Nicholls 1984; Benek et al. 1996; Geißler et al. 2008; Mattern 2001; Awdankiewicz et al. 2004; Neumann et al. 2004; Schmiedel et al. 2015; Repstock et al. 2018; Luthardt et al. 2018). Evidences of these events are major volcanic complexes as well as numerous volcano-sedimentary successions. In close proximity of the Döhlen Basin, the allochthonous domain of the Saxo-Thuringian Zone features the Chemnitz Basin (Schneider et al. 2012), the Tharandt Caldera (Benek 1980), and Teplice-Altenberg Volcanic Complex (Hoffmann et al. 2013; Walther et al. 2016), whereas the autochthonous domain inherits the North Saxon Volcanic Complex (Repstock et al. 2018; Röllig 1976). The Elbe Zone as a tectonic lineament comprises the Meissen Volcanic Complex and the Döhlen Basin (Fig. 2). Compared to most other Central European Permo-Carboniferous basins, the Döhlen Basin crosscuts the Variscan structures in NW–SE direction oriented parallel to the Elbe Zone (Schneider and Romer 2010).

Geology of the Döhlen Basin

The post-Variscan (Lowermost Permian) rearrangement of the stress field in Central Europe led to the formation of transtensional valleys (Schneider and Romer 2010). As a result, one of these, the Döhlen Basin formed. The basin is located in the Elbe Zone SE of the Meissen Massif and consists of in total c. 800 m thick successions of sedimentary and magmatic rocks that are partially covered by Mesozoic and Cenozoic sediments (Reichel 1970). The originally thicker sediments were affected partially by post-Rotliegend erosion (Reichel and Schauer 2006). Simultaneous to the sedimentation, extensive tectonics took place (Hoffmann 2000). The basin fill comprises pyroclastic rocks like ash-fall tuffs and ignimbrites as well as sandstones and limestones, whereas the NW part is dominated by andesitic to dacitic extrusive rocks (Hoffmann 2000; Reichel and Schneider 2012; Hoffmann et al. 2013). The sediments of the basin overlie Cadomian gneisses of the Erzgebirge and low-grade metamorphics of the Elbe Valley and Nossen-Wilsdruff Slate Complexes well as Variscan monzonites of the Meissen Massif. A NW–SE directed subdivision into a main depression of Döhlen and a side depression of Hainsberg-Quohren and Kohlsdorf-Pesterwitz exists. Due to several tectonic reactivations of the surrounding area, the basin fill of the Döhlen Basin comprises four megacycles of deposition (Schneider

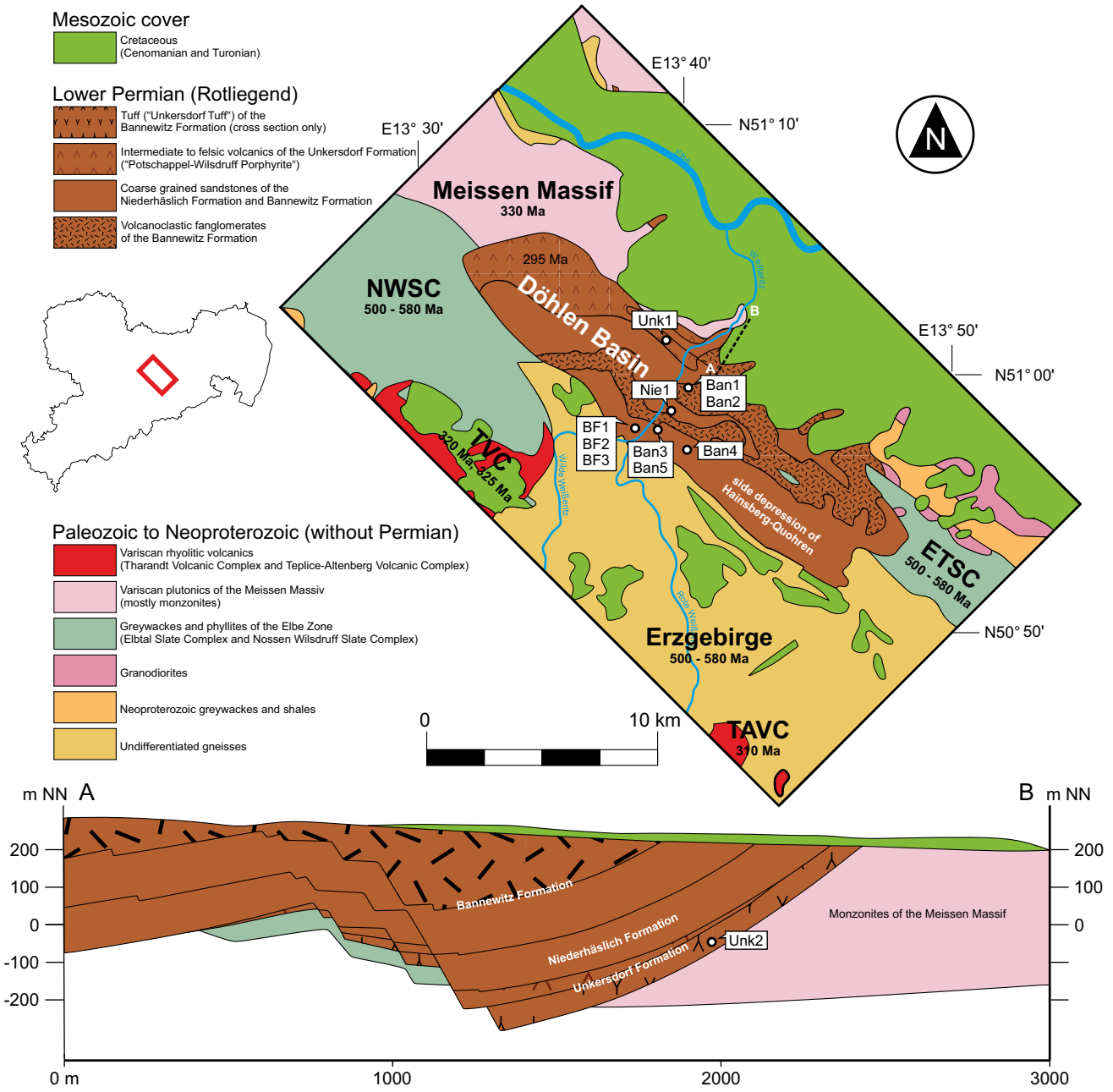

Fig. 2 Simplified geological map of the Döhlen Basin (Cenozoic cover removed) and adjoining areas modified after Alexowsky and Leonhardt (1994). Cross section A–B of the NE part of the Döhlen Basin (modified after Pietzsch 1963). *NWSB* Nossen-Wilsdruff schist belt, *ETSB* Elbtal Slate Complex, *TVC* Tharandt Volcanic Complex, *TAVC* Teplice-Altenberg Volcanic Complex. In the map all sample locations are indicated: Unk1, sample of a rhyodacitic lava from the Unkersdorf Formation; Unk2, sample of an intermediate tuff (Unkersdorf Tuff) from the Unkersdorf Formation (cross section only); Nie1, sample of a sandstone from the Niederhäslich Formation; Ban1 and Ban2, samples of the volcanic rock fanglomerates from the Bannewitz Formation; Ban3 and Ban 5, samples from a sandstone of the Bannewitz Formation; Ban4, sample of a felsic tuff (Wachtelberg ignimbritic tuff) from the Bannewitz Formation; BF1 and BF2, samples of a bended sandstone ('Gebänderte Feinklastite') from the Bannewitz Formation; BF3, sample of a gneiss rhyolite conglomerate from the Bannewitz Formation

and Hoffmann 2001, Figs. 3, 4). From the base to the top, the Döhlen Basin contains the Unkersdorf Formation, the Döhlen Formation, the Niederhäslich Formation and the Bannewitz Formation (see Fig. 3).

The up to 220 m thick Unkersdorf Formation started with the sedimentation of coarse basal conglomerates and basal breccias with a mean thickness of 5 m (Reichel 1970), with sometimes block-sized monzonite clasts

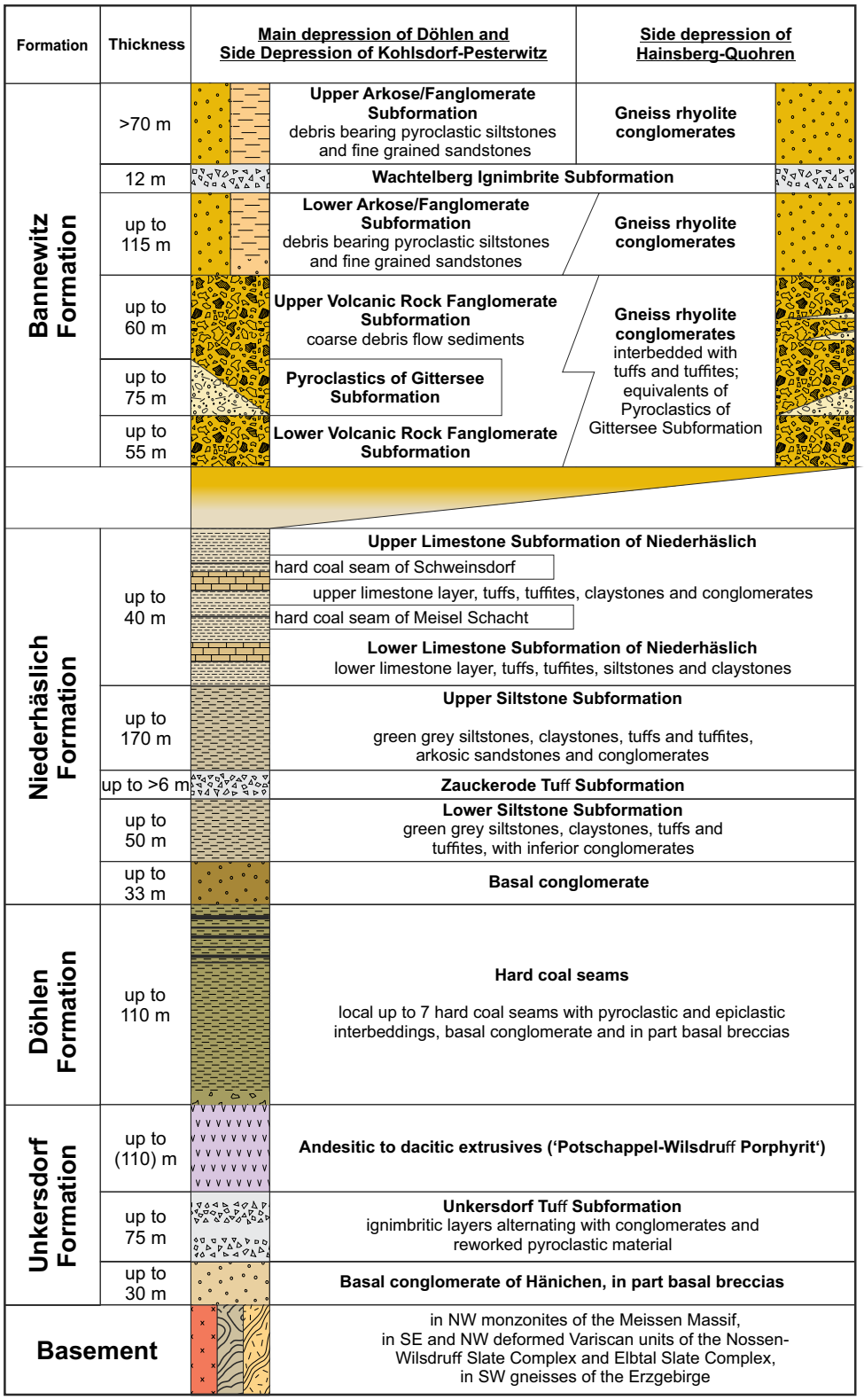

Fig. 3 Idealized section of the Döhlen Basin (modified after Reichel 1970)

(Reichel and Schneider 2012). After that, rhyodacitic pyroclastics, e.g., the Unkersdorf Tuff and siliciclastic sediments with a thickness of 75 m were deposited (Reichel and Schauer 2006). This subformation consists of tuffitic layers that are alternating with conglomerates. The pale to violet tuffites contains clasts of schist, sandstone, greywacke, andesite, porphyrite and monzonite (Reichel 1970; Hoffmann 2000; Hoffmann et al. 2013).

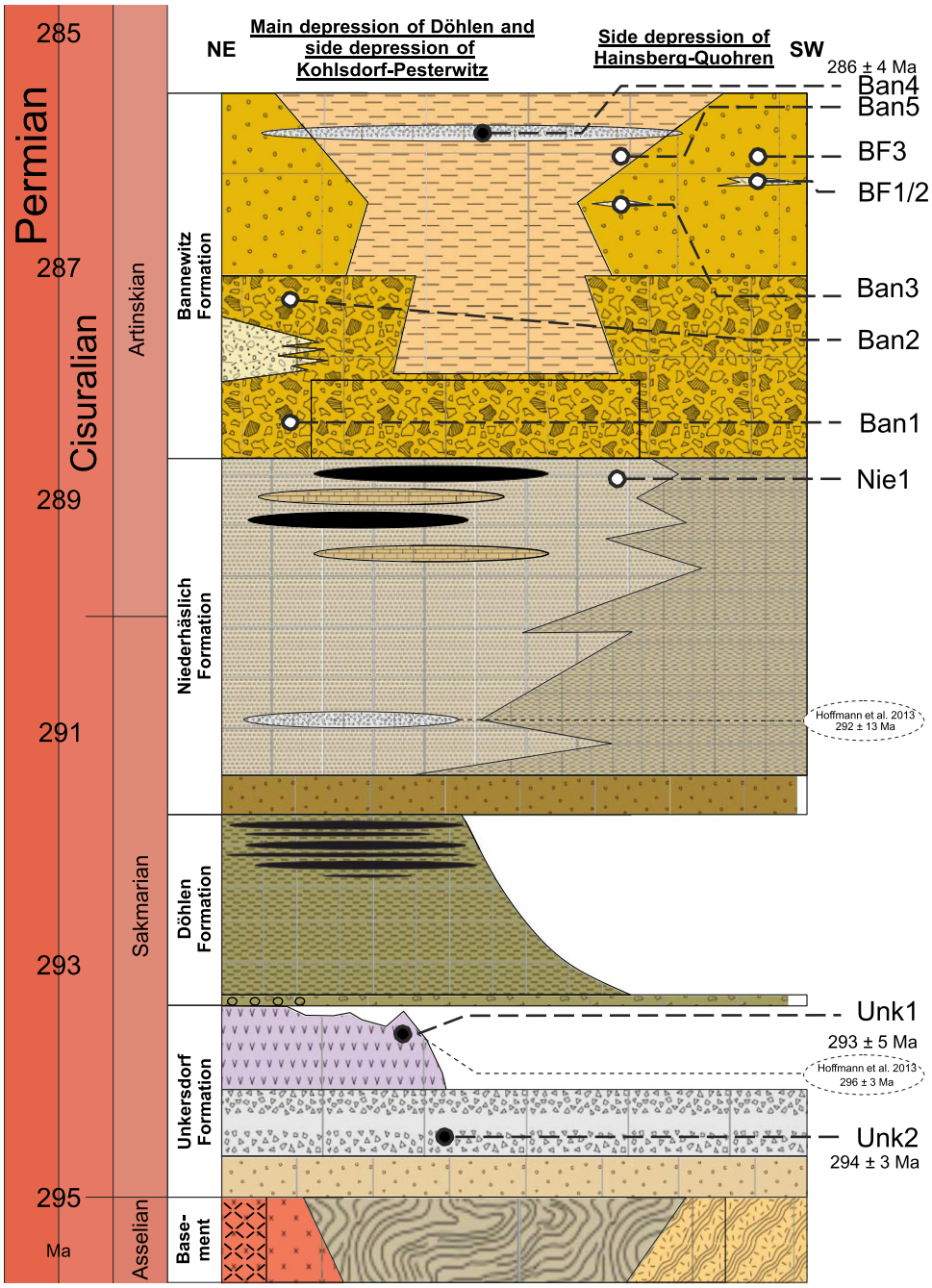

Fig. 4 NE–SW section of the Döhlen Basin with sample locations and calculated U–Pb ages (modified after Reichel 1970; Schneider and Hoffmann 2001; this paper). Patterns similar to Fig. 3. Note: black dots, magmatic samples; white dots, sedimentary samples

The heterogenic distribution of the clasts indicates a deposition by pyroclastic flows (Fisher and Schmincke 1984). Reichel and Lange (2007) suggested the Meissen Volcanic Complex as a possible source area. A violet gray andesitic to dacitic lava complex ('Potschappel Wilsdruff Porphyrit') covers the NW part of the Döhlen Basin with a maximum thickness of 80 m (Hoffmann and Schneider 2005). Schneider and Hoffmann (2001) suggested an Upper Carboniferous U–Pb zircon age. Hoffmann et al. (2013) reported a SHRIMP U/Pb age of 296 ± 3 Ma (Asselian) of the intermediate volcanic rocks.

Famous for its rich fossil records, coal, and uranium mining, the Döhlen Formation consists of alternating coarse clastic sediments, coal seams and tuffs (Fig. 3). The thickness of the formation fluctuates between 15 and 110 m (Reichel and Schneider 2012). Two fining-upward mesocycles whose deposits leveled up the paleorelief, are distinctive for the sedimentary record of the Döhlen Formation (Reichel 1970). Conglomerates, sand- and siltstones characterize the first cycle. In contrast, the second mesocycle can be divided into three to four minor cycles, which contain seven coal seams. Reworked air-fall deposits are intercalated

(Schneider and Hoffmann 2001). The occurring fine-grained sediments of the Döhlen Formation indicate a deposition as channels fills of fluvial systems (Reichel and Schauer 2006). In contrast, Reichel and Schneider (2012) suggest mainly palustrine depositional conditions. Both mesocycles are induced by a quick tectonic subsidence, whereas the minor cycles are likely defined by volcanic activity with large-scale air-fall deposits separating the coal seams (Reichel and Schauer 2006; Reichel and Schneider 2012). An indication for an increased tectonic activity is the occurrence of seismic dykes and traces of mass movements (Hausse 1892; Reichel 1970, 1985). Biostratigraphic ages given by Sterzel (1881, 1893) considered the age of the Döhlen Formation as Lower Rotliegend.

Conglomerates and sandstones with alternating grain size and a total thickness of c. 300 m are characteristic for the Niederhäslich Formation (Reichel and Schauer 2006). The formation is subdivided into (1) 33 m of basal conglomerate, (2) 30–50 m (lower) siltstones, (3) up to 6 m tuff, followed by (4) 130–170 m (upper) siltstones and on top up to (5) 40 m limestone (Reichel and Schauer 2006, Fig. 3). An increasing conglomerate portion from main to side depression can be observed (Fig. 4). The basal conglomerate consists mainly of rhyolite and paragneiss and includes layers of pebble-bearing coarse-grained sandstones (Reichel and Schneider 2012). The green-gray Lower Siltstones show a fluviatile to lacustrine origin (Schneider 1994), whereas the Upper Siltstones are made up of sandy siltstones, which consist of reworked pyroclastic material and show partially cross-bedding structures (Reichel and Schauer 2006). They contain embedded channels of coarse-grained sandstones and conglomerates, which are also present at the Lower Siltstone successions (Reichel and Schneider 2012). Between both of the siltstone layers, a pyroclastic deposit occurs, which is termed Zauckerode Tuff. The latter is a marker horizon throughout the main depression of Döhlen. Limestones are typical for the uppermost layer of the Niederhäslich Formation, which imply a general facies change (Reichel and Schneider 2012). The depositional conditions of the formation can be described as a shallow drainless basin with a braided river system (Schneider and Gebhardt 1992) whose ongoing sedimentation continuously covered the hinterland (Reichel and Schauer 2006). Playas or alluvial plain environments like the recent day Etosha Pan in Namibia could have been another possible scenario (Reichel and Schneider 2012). Werneburg and Schneider (2006) considered the Niederhäslich Formation as the uppermost Unterrotliegend in age based on biostratigraphic findings. Hoffmann et al. (2013) presented a Pb/Pb single zircon age of the Zauckerode Tuff at 292 ± 13 Ma. Disregarding the big error, it fits well with the given biostratigraphic age.

The red sediments of the Bannewitz Formation reach a thickness of 380 m. The deposits consist mainly of coarse-grained fanglomerates with a high portion of rhyolite and gneiss clasts. This formation differs in its characteristics between the (1) main depression of Döhlen and the side depression of Kohlsdorf-Pesterwitz and (2) the side depression of Hainsberg-Quohren (see Fig. 4). Whereas the first (Döhlen Basin, Kohlsdorf-Pesterwitz) is build up mainly by volcanic fanglomerates and arkose, the Hainsberg-Quohren depression contains mainly gneiss and rhyolite conglomerates. The Wachtelberg Ignimbrite is existent in both and therefore represents a marker horizon. The thickness of the Lower Volcanic Fanglomerate Subformation in the Döhlen and Kohlsdorf-Pesterwitz depressions ranges between 15 and 55 m. After Reichel (1970), these sediments were deposited by large debris flows entering the Döhlen Basin from the northwest. However, the center of the basin shows finer arkosic to conglomeratic sediments, which Schneider and Hoffmann (2001) interpreted as channel fillings of fan systems. The 20–60 m thick Upper Volcanic Fanglomerate Subformation differs from the Lower Volcanic Fanglomerate Subformation through alternating components of porphyrites and rhyolites (Neumann 1961). Between both subformations, the bedded Pyroclastics of Gittersee and equivalents with a thickness of c. 75 m are intercalated (Reichel and Schauer 2006; Reichel and Schneider 2012; Fig. 3). The Lower and Upper Arkose/Fanglomerate subformations were deposited in the central part of the basin. Both subformations show an abundant volcanic and minor metamorphic input that is indicated by the content of clasts (Neumann 1961; Hoffmann 2000). Reichel and Schauer (2006) consider the deposition on alluvial fans. The Lower and Upper Arkose/Fanglomerate subformations are separated by the 12 m thick marker horizon of the Wachtelberg Ignimbrite (Hoffmann 2000). The depositional environment may be described as lahar and/or alluvial fan (Reichel and Schauer 2006). Reichel and Schneider (2012) discuss a channel based reworking of some material of these strata. In contrast to the main depression of Döhlen and the side depression of Kohlsdorf-Pestewitz, the side depression of Hainsberg-Quohren consists only of gneiss and rhyolite conglomerates and shows no fanglomerates and arkoses. In the lower part of this side depression, these conglomerates are interbedded with tuffs and tuffites that are interpreted as equivalents of the pyroclastics of the Gittersee Subformation (Reichel and Schauer 2006). For the Bannewitz Formation, Schneider and Hoffmann (2001) suggests a Lower to Upper Rotliegend age, whereas Reichel and Schauer (2006) suggest a Lower Rotliegend age.

Methods

Zircon concentrates were separated from 2 to 4 kg sample material at the Senckenberg Naturhistorische Sammlungen Dresden (Museum für Mineralogie und Geologie) using

standard methods. Final selection of the zircon grains for U–Pb dating was achieved by hand-picking under a binocular microscope. Zircon grains of all grain sizes and morphological types were selected, mounted in resin blocks and polished to half their thickness. Zircons were analyzed for U, Th, and Pb isotopes by LA-SF ICP-MS techniques at the Senckenberg Naturhistorische Sammlungen Dresden (Museum für Mineralogie und Geologie), using a Thermo-Scientific Element 2 XR sector field ICP-MS (single-collector) coupled to a New Wave UP-193 Excimer Laser System. A teardrop-shaped, low volume laser cell constructed by Ben Jähne (Dresden) and Axel Gerdes (Frankfurt/M.) was used to enable sequential sampling of heterogeneous grains (e.g., growth zones) during time-resolved data acquisition. Each analysis consisted of approximately 15 s background acquisition followed by 30 s data acquisition, using a laser spot size of 25 and 35 µm, respectively. A common Pb correction based on the interference- and background-corrected ^{204}Pb signal and a model Pb composition (Stacey and Kramers 1975) was carried out if necessary. The necessity of the correction is judged on whether the corrected ^{207}Pb/^{206}Pb lies outside of the internal errors of the measured ratios (Frei and Gerdes 2009). Discordant analyses ranging from 90 to 103% were generally interpreted with care with respect to the internal structure of the respective zircon grain. Raw data were corrected for background signal, common Pb, laser-induced elemental fractionation, instrumental mass discrimination, and time-dependant elemental fractionation of Pb/Th and Pb/U using an Excel® spreadsheet program developed by Axel Gerdes (Institute of Geosciences, Johann Wolfgang Goethe University Frankfurt, Frankfurt am Main, Germany). Reported uncertainties were propagated by quadratic addition of the external reproducibility obtained from the standard zircon GJ-1 (~0.6% and 0.5–1.0% for the ^{207}Pb/^{206}Pb and ^{206}Pb/^{238}U, respectively; Jackson et al. 2004) during individual analytical sessions and the within-run precision of each analysis. The total offset of the measured drift-corrected ^{206}Pb*/^{238}U ratio from the "true" ID-TIMS value (0.0986 ± 0.16%; ID-TIMS value) of the analyzed GJ-1 grain was between 3 and 12% (during all analytical sessions) and the drift over the day, during the different analytical sessions between 1 and 8%. To test the accuracy of the measurements and data reduction, we included the Plesovice zircon as a secondary standard in our analyses. Repetitive measurements over the last years of the Plesovice zircon resulted in the age of 337.3 ± 1.2 Ma, which fits the results of Slama et al. (2008). Concordia diagrams (2σ error ellipses) and concordia ages (95% confidence level) were produced using Isoplot/Ex 2.49 (Ludwig 2001) and frequency and relative probability plots using AgeDisplay (Sircombe 2004). The ^{207}Pb/^{206}Pb age was taken for interpretation of all zircons > 1.0 Ga, and the ^{206}Pb/^{238}U ages for younger grains. Further details of the instruments settings are available in the Supplementary Material. For further details on analytical protocol and data processing see Gerdes and Zeh (2006). Detrital zircons showing a degree of concordance in the range of 90–103% in this paper are classified as concordant because of the overlap of the error ellipse with the concordia. Zircon U–Pb analyses used for calculating Concordia ages were derived from analyses with a degree of concordance between 98 and 102%, to exclude lead loss effects during age calculation. Th/U ratios are obtained from the LA-ICP-MS measurements of investigated zircon grains. U and Pb content and Th/U ratio were calculated relative to the GJ-1 zircon standard and are accurate to approximately 10%. Analytical results of U–Th–Pb isotopes and calculated U–Pb ages are given in the Supplementary Material. Concerning stratigraphic ages, the stratigraphic time scale of Gradstein et al. (2012) had been used.

Hafnium isotope measurements were taken with a Thermo-Finnigan NEPTUNE multi-collector ICP-MS at Institute of Geosciences, Johann Wolfgang Goethe University Frankfurt, Frankfurt am Main, Germany coupled to RESOlution M50 193 nm ArF Excimer (Resonetics) laser system following the method described in Gerdes and Zeh (2006, 2009). Spots of 40 µm in diameter were drilled with a repetition rate of 4.5–5.5 Hz and an energy density of 6 J/cm^2 during 50 s of data acquisition. The instrumental mass bias for Hf isotopes was corrected using an exponential law and a 179Hf/177Hf value of 0.7325. In the case of Yb isotopes, the mass bias was corrected using the Hf mass bias of the individual integration step multiplied by a daily βHf/βYb offset factor (Gerdes and Zeh 2009). All data were adjusted relative to the JMC475 of 176Hf/177Hf ratio = 0.282160 and quoted uncertainties are quadratic additions of the within-run precision of each analysis and the reproducibility of the JMC475 (2SD = 0.0028%, n = 8). Accuracy and external reproducibility of the method was verified by repeated analyses of reference zircon GJ-1 and Plesovice, which yielded a 176Hf/177Hf of 0.282007 ± 0.000026 (2SD, n = 42) and 0.0282469 ± 0.000023 (n = 20), respectively. This is in agreement with previously published results (e.g., Gerdes and Zeh 2006; Slama et al. 2008) and with the LA-MC-ICP-MS long-term average of GJ-1 (0.282010 ± 0.000025; n > 800) and Plesovice (0.282483 ± 0.000025, n > 300) reference zircon at Institute of Geosciences, Johann Wolfgang Goethe University Frankfurt, Frankfurt am Main, Germany.

The initial ^{176}Hf/^{177}Hf values are expressed as $_{\varepsilon}$Hf(t), which is calculated using a decay constant value of 1.867×10^{-11} year^{-1}, CHUR after Bouvier et al. (2008; ^{176}Hf/^{177}Hf$_{\mathrm{CHUR,\ today}}$ = 0.282785 and ^{176}Lu/^{177}Hf$_{\mathrm{CHUR,today}}$ = 0.0336) and the apparent U–Pb ages obtained for the respective domains (Supplementary Data). For the calculation of Hf two-stage model ages (T_{DM}) in billion years, the measured ^{176}Lu/^{177}Lu of each spot (first stage = age of zircon), a value of 0.0113 for the average continental crust,

and a juvenile crust $^{176}Lu/^{177}Lu_{NC} = 0.0384$ and $^{176}Hf/^{177}Hf$ NC = 0.283165 (average MORB; Chauvel et al. 2007) were used.

The geochemical analyses of the rock samples had been done by FUS-ICP and FUS-MS and were carried out by Actlabs in Ancaster (Ontario, Canada).

Results

Magmatic samples (Unk1, Unk2, Ban4)

For the three magmatic samples of this study, we analyzed in total 170 zircon grains of which 103 yielded a concordant age within the rage of 90–103% degree of concordance. The sample Unk1, a violet to gray trachyandesite (Unkersdorf Formation) was sampled in the city area of Freital at the top of the Burgwartsberg. It contained eight zircon grains. Five of them yielded concordant ages representing two groups with distinct Concordia ages (1) between c. 290 ± 9 Ma and 296 ± 11 Ma (three analyses) and (2) ranging from c. 560 ± 17 Ma to 569 ± 19 Ma (two analyses). A Concordia age calculated for the three youngest grains is given at 293 ± 5 Ma that is interpreted as the cooling age (see Figs. 5, 6a; Supplementary Data).

Sample Unk2 (bedded violet tuff, Unkersdorf Formation) was collected in an abandoned mining shaft of the quarry Osterberg near the Weißeritz river in Freital. The sample featured in total 42 zircon grains with 16 of them being concordant in the range of 90–103% of concordance between 290 ± 12 and 332 ± 10 Ma and 1 grain with a Mesoproterozoic age of 1449 ± 49 Ma. The calculated Concordia age for the nine youngest grains results in an age of emplacement for the tuff at 294 ± 3 Ma (see Figs. 5, 6b; Supplementary Material).

We analyzed 120 zircons of the violet to gray Wachtelberg ignimbritic tuff (Ban4, Upper Bannewitz Formation), which was sampled as a cobble on a field between the city Freital and village Cunnersdorf. Eighty-two grains of them were considered as concordant within the range of 90–103% of concordance. The calculated ages range from 284 ± 9 to 620 ± 35 Ma. In addition, one Mesoproterozoic age at 1127 ± 23 Ma was found. The Concordia plot of the five youngest grains shows an emplacement age of 286 ± 4 Ma (see Figs. 5, 6c; Supplementary Data).

Sedimentary samples (Nie1, Ban1, Ban2, Ban3, Ban5, BF1, BF2, BF3)

We analyzed in total 984 zircon grains from 8 sedimentary samples, 533 showed a degree of concordance between 90 and 103% and were regarded as concordant. Figure 9 shows the U–Pb dataset of all analyzed detrital zircons of this study between 200 and 750 Ma.

All analyzed sediments but two show two distinct age clusters: (1) between 295 and 340 Ma (Variscan) and (2) between 530 and 750 Ma (Cadomian). Despite this general similarity among the samples, the total and relative amount of concordant (90–103%) analyses for each age group varies strongly. There is a lack of ages between both age clusters (see Fig. 7) for all sedimentary samples. Only the samples Ban2 and Ban 5 show very few ages in the range of 370–470 Ma, while all other sediments are characterized by a complete absence of ages falling into the latter age range. Beside samples BF1, BF2 and Ban5 all samples show sporadic ages > 1.0 Ga (Fig. 5). Sample Ban3 also yields two Archean ages.

Sandstone Nie1 (oldest of all analyzed sediments) of the Niederhäslich Formation was collected at the riverbank of the Weißeritz in Freital. The sample shows high amounts of Cadomian ages (76%) and low amounts of Variscan ages (14%). Both samples of the volcanic rock fanglomerates (Lower Bannewitz Formation) were sampled at the bottom (Ban1) and top (Ban2) of the Windberg (Freital). The red fanglomerates comprise big clasts of angular, internally foliated rhyolites and well-rounded rhyolites containing almost only Variscan zircon ages (85% and 65%, respectively). Sample Ban3 (equivalent of the pyroclastics of Gittersee in the side depression of Hainsberg-Quohren) was collected at the riverbank of the Weißeritz near the 'Schweinsdorfer Alpen' in Freital. The red, coarse-grained sandstone contained decimeter-sized clasts of well-rounded rhyolites and gneiss. The age composition for latter sample is very different from sample Ban5 with a majority of Cadomian ages (about 70%) and only a few Variscan ones (4%, see Fig. 8). The overlying Upper Arkose/Fanglomerate Subformation represented by sample Ban5 (red, coarse-grained sandstone Upper Bannewitz Formation, small clasts of gneiss) were collected above sample Ban3 at the top of the 'Schweinsdorfer Alpen' in Freital and gave 48% Variscan ages and 38% Cadomian ages. In contrast, samples BF1, a gray conglomerate with decimeter-sized clasts of well-rounded rhyolites, angular-foliated rhyolites and gneiss, sample BF2, a red sandstone, of the equivalents of the pyroclastics of Gittersee, and sample BF3, a reddish cray conglomerate with decimeter-sized clasts of well-rounded rhyolites and gneiss of the gneiss rhyolite conglomerate show detrital zircon age patterns with nearly equal amounts of Variscan and Cadomian U–Pb ages. All of the latter three samples are part of the Bannewitz Formation and were collected at the Backofenfelsen in Freital.

A summary of all samples investigated for this study including zircon sizes and morphology is given in in Table 1.

Out of 120 U–Pb zircon measurements for sample Nie1 (gray, coarse-grained sandstone; Niederhäslich Formation),

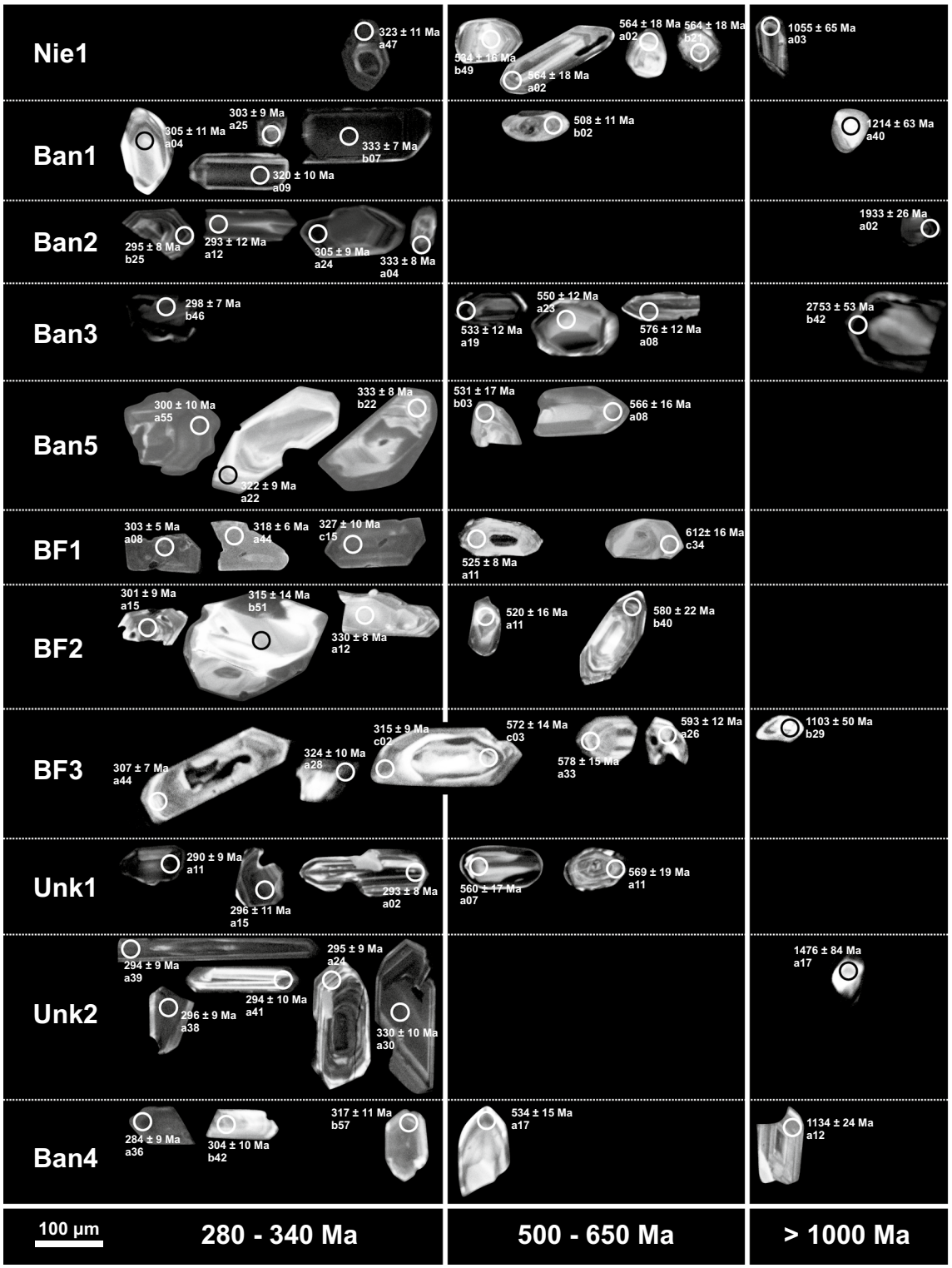

Fig. 5 Selected cathodoluminescence images of zircon grains representing the main age groups for all samples. Circles indicating the laser spots with a diameter of 25 µm. For every spot, the U–Pb age is given with the 2σ error in Ma. Note spots c02 and c03 from sample BF3 show concordant ages of a complex zircon grain

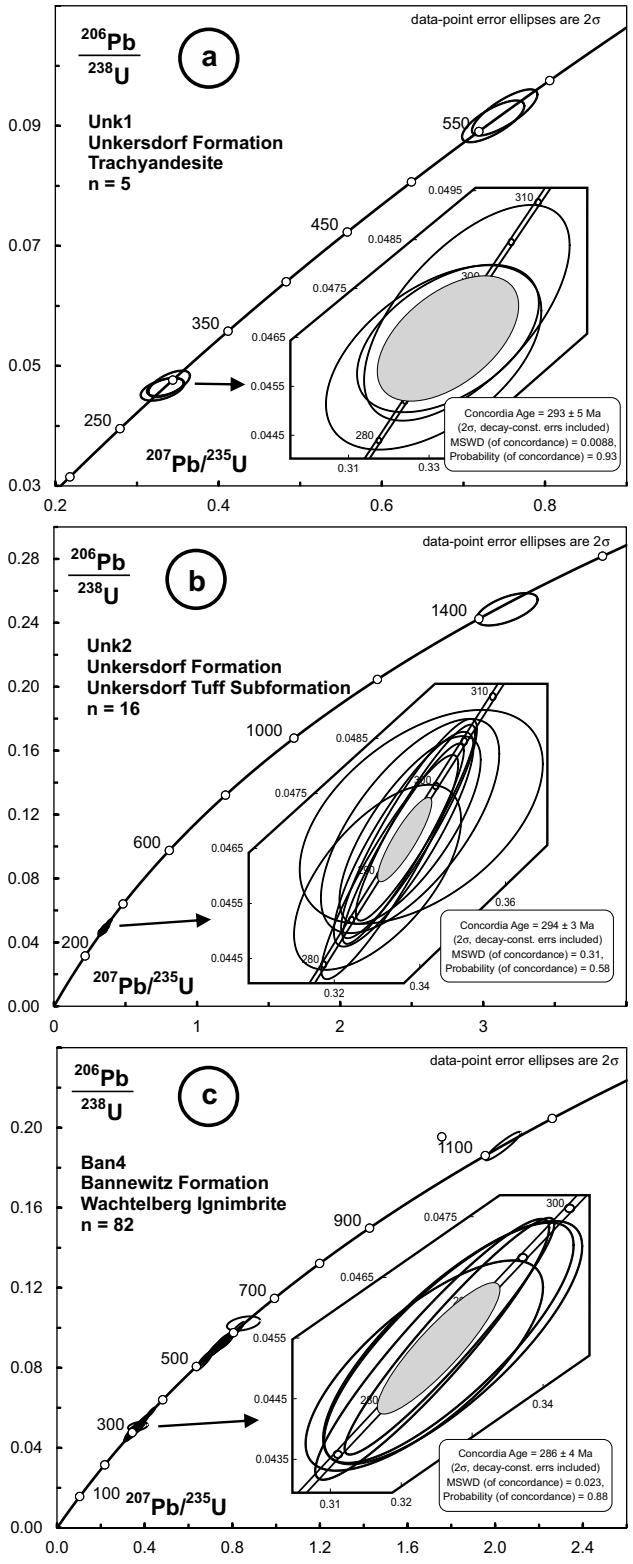

Fig. 6 Concordia plots of all analyzed magmatic zircons (three samples). **a** Concordia plot of sample Unk1 (trachyandesitic lava) and the U–Pb ages of the three youngest zircon grains and the calculated age of sample Unk1. **b** Concordia plot of sample Unk2 (tuff) and the U–Pb ages of the nine youngest zircon grains and the calculated age of sample Unk2. **c** Concordia plot of all analyzed zircons of sample Ban4 (Wachtelberg Ignimbrite) and the U–Pb ages of the five youngest zircon grains and the calculated age of sample Ban4

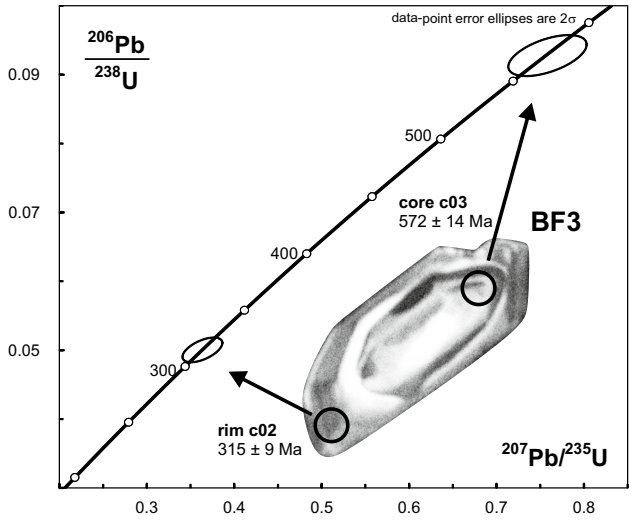

Fig. 7 Concordia plot (2σ error ellipses) of one complex zircon grain of sample BF3 showing an old core and a younger rim. The grain reflects Cadomian (core) and Variscan (rim) growth events, which can be seen in all other samples of this study typical for the Saxo-Thuringian Zone. Scale: laser spots 25 µm in diameter. Diagrams are based on data given in Supplementary Data

58 provided concordant ages within the range of 90–103% of concordance. Noticeable is the major amount of Cadomian zircon ages and the minor amount of Variscan ages. In addition, there are some Devonian, Upper Ordovician and Upper Cambrian as well as Mesoproterozoic and Paleoproterozoic ages (Figs. 5, 8; Supplementary Data).

Samples Ban1 and Ban2 were taken from the Lower and Upper Volcanic Rock Fanglomerates of the Bannewitz Formation. We analyzed 116 (Ban1) as well as 106 (Ban2) detrital zircon grains. Thereof 75 (Ban1) and 46 (Ban2) measurements showed a degree of concordance between 90 and 103%. Both samples provided mainly Variscan U–Pb ages and show peaks at 305, 315, 325 and 340 Ma. Sporadic Carboniferous, Neoproterozoic, Mesoproterozoic and Paleoproterozoic ages occur (Figs. 5, 8; Supplementary Data).

We measured 120 detrital zircons of sample Ban3 of the Upper Bannewitz Formation with respect to their U–Pb composition. Ninety-five of them show a degree of concordance between 90 and 103%. A significant amount of the measurements gave Cadomian U–Pb ages. Only a minor amount (4%) feature Variscan ages. The sample revealed also Ordovician, Paleoproterozoic and Archaic ages (Figs. 5, 8; Supplementary Data).

Of the 120 zircon age measurements of sample, Ban5 69 gave a concordant age (90–103% of concordance). Compared to sample Ban1, 2 and 3, the age distribution differs. Both, Cadomian and Variscan ages, represent significant age peaks with nearly equal amount of U–Pb ages. There are peaks at 310 and 320 Ma. Remarkable is the absence of ages > 1.0 Ga (Figs. 5, 8; Supplementary Data).

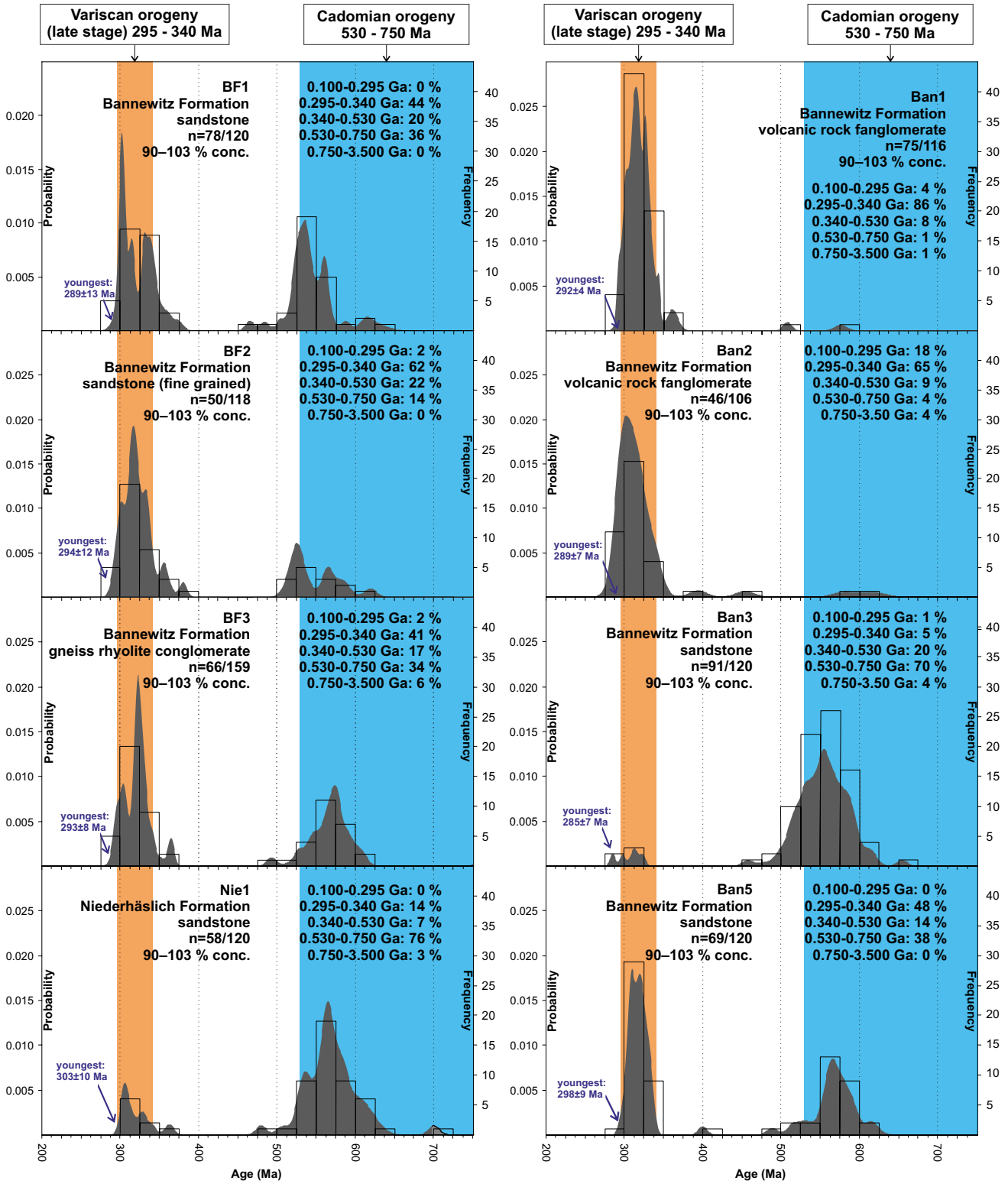

Fig. 8 Combined binned frequency and probability density distribution plots of all analyzed concordant (90–103%) detrital zircons (eight samples) of the Döhlen Basin with an age between 200 and 750 Ma using AgeDisplay (Sircombe 2004). Diagrams are based on data given in Supplementary Data

Table 1 Summary of samples investigated for this study

Sample	Lithology	Locality	Stratigraphic unit	Facies	Size of zircons (µm)	Morphology of zircons
Unk1	Traychyandsite	N51°01′02.8″ E13°39′07.3″	Unkersdorf Formation	–	Length: 204.3–258.4 Width: 131.3–87.7	Short prismatic crystals, bypyramidal faces and simple facets, some rounded grains
Unk2	Tuff	–	Unkersdorf Formation	Bedded violet tuff	Length: 70.2–236.1 Width: 50.7–160.8	Long and short prismatic crystals, bypyramidal faces and simple facets
Nie1	Sandstone	N50°59′16.9″ E13°38′43.6″	Niederhäslich Formation	Bedded medium-grained gray arcosic sandstone	Length: 71.8–231.3 Width: 40.6–97.8	Short prismatic crystals, bypyramidal faces and simple facets, many rounded grains
Ban1	Fanglomerate	N50°59′54.7″ E13°39′29.2″	Bannewitz Formation	Massive pale yellow to pinkish fanglomerate with centimeter-sized clasts of flow-structured porphyrites	Length: 73.6–315.1 Width: 52.7–90.9	Long prismatic crystals, bypyramidal faces and simple facets
Ban2	Fanglomerate	N50°59′49.0″ E13°39′38.4″	Bannewitz Formation	Massive pale yellow to pinkish fanglomerate with centimeter-sized clasts of flow-structured porphyrites	Length: 72.4–241.7 Width: 44.7–67.6	Short prismatic crystals, bypyramidal faces and simple facets
Ban3	Sandstone	N50°59′01.5″ E13°38′14.2″	Bannewitz Formation	Bedded reddish coarse-grained sandstone with few decimeter-sized clasts of gneiss and rounded rhyolite	Length: 55.0–147.1 Width: 44.0–87.3	Short prismatic crystals, bypyramidal faces and simple facets
Ban4	Ignimbritic tuff	N50°58′34.3″ E13°39′27.2″	Bannewitz Formation	Gray to violet massive untextured ignimbritic tuff	Length: 58.9–189.0 Width: 44.3–104.4	Short prismatic crystals, bypyramidal faces and simple facets
Ban5	Sandstone	N50°59′01.0″ E13°38′19.9″	Bannewitz Formation	Bedded reddish fine-grained sandstone	Length: 53.8–302.1 Width: 34.2–140.4	Short prismatic crystals, bypyramidal faces and simple facets
BF1	Sandstone	N50°58′58.9″ E13°37′47.5″	Bannewitz Formation	Massive red fine-grained sandstone	Length: 49.0–188.1 Width: 26.4–65.7	Short prismatic crystals, bypyramidal faces and simple facets
BF2	Sandstone	N50°58′58.9″ E13°37′47.5″	Bannewitz Formation	Massive white coarse-grained sandstone with few decimeter-sized clasts of gneiss and rounded rhyolite	Length: 70.2–183.9 Width: 25.5–55.1	Short prismatic crystals, bypyramidal faces and simple facets
BF3	Conglomerate	N50°59′00.4″ E13°37′47.3″	Bannewitz Formation	Massive reddish conglomerate with centimeter-sized clasts	Length: 29.4–137.0 Width: 29.4–44.9	Short prismatic crystals, bypyramidal faces and simple facets, many rounded grains

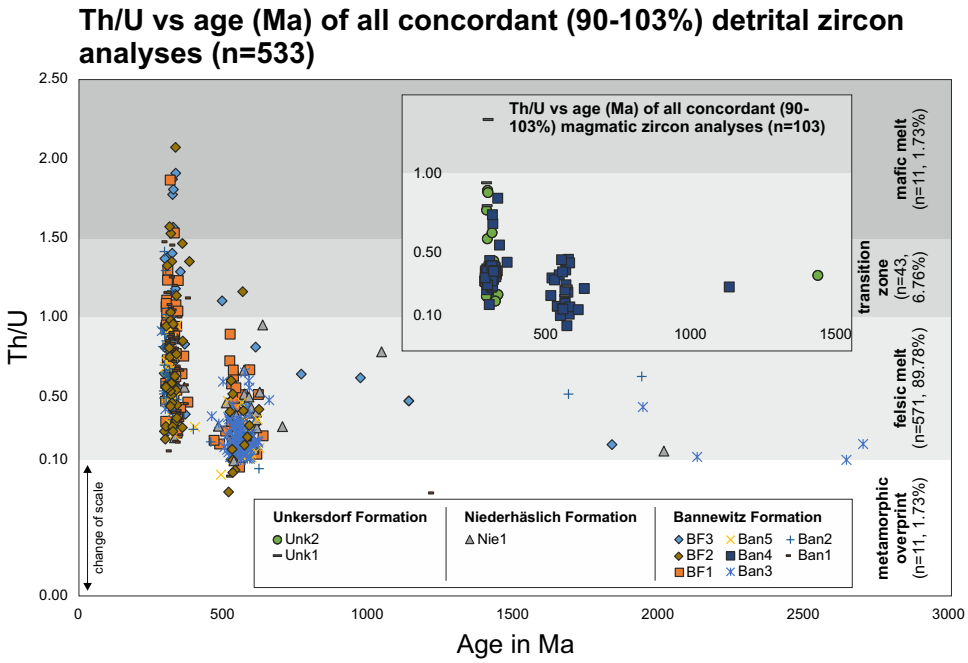

Fig. 9 Th/U vs zircon age diagram of all analyses, separated in detrital and magmatic (inset) samples, with a degree of concordance within 90–103%, showing that all zircons were derived mainly from felsic melts. Only a minority of eleven grains show evidence of mafic melts (Th/U ratios above 1.50). Eleven grains show Th/U ratios below 0.1, which indicates a significant metamorphic overprint. The diagram is based on the Th/U ratios given in Supplementary Data

For BF1 67 of 119 measurements, for BF2 50 of 119 measurements, and for BF3 66 of measured 159 spots were concordant in the range of 90–103% of concordance. All three samples show similar age patterns with a majority of Variscan ages and a large group of Cadomian ages. Variscan peaks at 305, 325 and 340 Ma are present. Similar to sample Ban5, the samples BF1 and BF2 show no ages > 1.0 Ga, whereas sample BF3 yields several Mesoproterozoic and Paleoproterozoic ages (Figs. 5, 8; Supplementary Data). One complex zircon grain of sample BF3 featured a Cadomian core and a Variscan rim with ages of 572 ± 14 Ma and 315 ± 9 Ma, respectively (Fig. 7).

Th/U isotope ratios, Hf isotopic and geochemical data

The obtained Th/U ratios are below 1.0 for the majority (90%) of all analyzed zircon grains with concordant U–Pb age, which points to a felsic melt composition (Wang et al. 2011). Besides, there is a minor zircon population of eleven grains (2%) with Th/U ratios below 0.1. This is an indication for a strong metamorphic overprint (e.g., Hoskin and Schaltegger 2003; Linnemann et al. 2007). In addition, a relatively small amount of 43 grains (6%) ended up in a 'transition zone' with no clear correlation to either felsic or mafic melt. Only eleven grains (2%) tend towards a melt of mafic origin (Wang et al. 2011; Fig. 9).

εHf(t) values of 299 analyses show a wide variety and range from −29.8 to 5.8, with a cluster of mainly Mesoproterozoic to Paleoproterozoic $T_{(DM)}$ model ages (Fig. 10; Table 2, Supplementary Data). This implies a mixing of melts of younger Variscan with older Precambrian Cadomian crust. The latter is composed of Ediacaran to Upper Cryogenian (c. 570–650 Ma) and 2.0–3.4 Ga old West African Craton components (Gerdes and Zeh 2006). During formation of Döhlen Basin zircons, a reworking of a Variscan crustal source occurred. The data did not show any evidence for an involvement of juvenile crust (Fig. 10).

Figure 11a–e and Supplementary Table 3 provides the results of the geochemical analyses. According to the REE pattern (Fig. 11a), all samples but Ban1, Ban2 and Unk1 feature a negative Europium anomaly, which may either point towards a felsic provenance (evolved crustal source) of the sediments or a mantle magma source. A felsic source corroborates with the Th/U ratios and the majority of negative εHf(t) values (Figs. 9, 10). The volcanic rock sample Unk1 falls into the trachyandesite field of the total alkali vs silica (TAS) diagram of Le Maitre et al. (1989) for volcanic rocks (Fig. 11b). Furthermore, the log (K_2O/Na_2O) vs SiO_2 discrimination diagram of Roser and Korsch (1986) of all sediment samples shows a trend towards an active continental margin and also an environment promoting strike-slip basins, merely samples Nie1 and Ban1 show a trend towards a passive margin signature (Fig. 11c). The discrimination diagrams of Al_2O_3/SiO_2 vs $Fe_2O + MgO$ (Bhatia 1983, Fig. 11d) and Th-Sc-Zr/10 (Bhatia and Crook 1986, Fig. 11e) show similar results. Thus, all sediment samples tend towards an active continental margin setting and/or possible strike-slip tectonics (Fig. 11d, e).

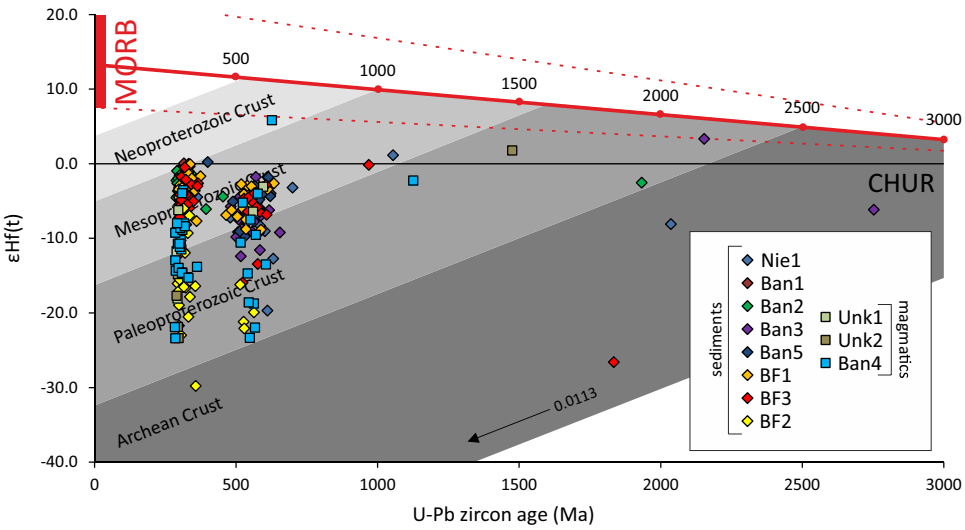

Fig. 10 $_{\varepsilon}$HF(t) versus age diagram of selected magmatic zircon grains and literature data. The continental crust evolution trends of the main components of the West African Craton and the Cadomian orogen are shown in different gray scales. See text for discussion

Discussion

Evolution of the Döhlen Basin as part of the post-Variscan tectonic activation of Central Europe

Based on the obtained U–Pb ages from magmatic zircon grains of the Döhlen Basin (samples Unk1, Unk2 and Ban4), both the initial and the end phase of the basin development are possible to be determined. Disregarding the basal conglomerate of the Unkersdorf Formation, the Unkersdorf Tuff (sample Unk2) marks the onset of the first basin deposits (Figs. 3, 4). The analyzed magmatic zircons reflect a Lower Asselian to Sakmarian age of 294 ± 3 Ma (Fig. 6b), which we consider as the age of the initial forming of the Döhlen Basin. Shortly after the major tuffitic depositions of the Unkersdorf Tuff Subformation, trachyandesitic to rhyodacitic lavas ('Potschappel Wilsdruff Porphyrites') occurred. The U–Pb data of sample Unk1 (trachyandesite, Fig. 11b) shows a slightly younger emplacement age of 293 ± 5 Ma (Sakmarian; Fig. 6a), which corresponds within the error with the obtained age of 296 ± 3 Ma by Hoffmann et al. (2013). An Upper Carboniferous age estimated by Schneider and Hoffmann (2001) for the Unkersdorf Formation based on biostratigraphic constraints is somewhat problematic, as it does not even fit within error to any of our data.

The ignimbritic tuff (sample Ban4) of the uppermost part of the Bannewitz Formation and therefore also from the uppermost part of the sedimentary succession of the Döhlen Basin (Fig. 4) gave an age of 286 ± 4 Ma and marks the final stage of basin development (Middle Artinskian to Lower Kungurian; Fig. 6c). Considering the errors of the lower- and uppermost ages, the evolution of the Döhlen Basin lasted till a maximum of 15 Ma, while a much shorter time range of about 8 Ma is suggested by the mean ages. This goes along with the Upper Asselian to Lower Kungurian formation proposed by Reichel and Schneider (2012).

With our data, it is also possible to correlate the evolutionary stages of the Döhlen Basin with several phases of post-Variscan activation in Central Europe. The increased magmatism during the formation of the Unkersdorf Formation at the base of the Döhlen Basin may be linked to a phase of high basic to intermediate magmatism at the Asselian/Sakmarian boundary (Schneider et al. 1995). Besides the Döhlen Basin, the Chemnitz Basin and the North Saxon Volcanic Complex features lowermost Permian ages and intermediate volcanics, too (Hoffmann et al. 2013; Luthardt et al. 2018; Rößler et al. 2009). Other Central European Permo-Carboniferous Basins like the Saar-Nahe Basin (Lorenz and Haneke 2004), the Thuringian Forest Basin (Obst et al. 1999) and the Flechtingen-Roßlau Block (Breitkreuz and Kennedy 1999; Breitkreuz et al. 2007) give evidence of basic to intermediate volcanism between c. 300 and 292 Ma. The volcanic peak coincides with the change from convergent plate tectonics to strike-slip dominated tectonics in Central Europe (Arthaud and Matte 1977; Linnemann and Schauer 1999; Heeremans et al. 2004). In addition, the discrimination diagrams for the sediments of the Döhlen Basin are indicating strike-slip tectonics and an associated basin development (Bhatia and Crook 1986; see Fig. 11c–e). The final stage of the evolution of the Döhlen Basin may be linked to a second culmination of volcano-tectonic activity accompanied with volcanic eruption and deposition of coarse clastic sediments at the Lower Rotliegend to Upper Rotliegend I boundary (Schneider et al. 1995).

Since $_{\varepsilon}$Hf(t) values of the investigated zircons mainly indicate Meso- to Paleoproterozoic $T_{(DM)}$ ages, we propose a recycling and mixing of Variscan with older Cadomian crust during the lower Permian peak of volcanism (Fig. 10). The Cadomian basement (Erzgebirge, Nossen-Wilsdruff and

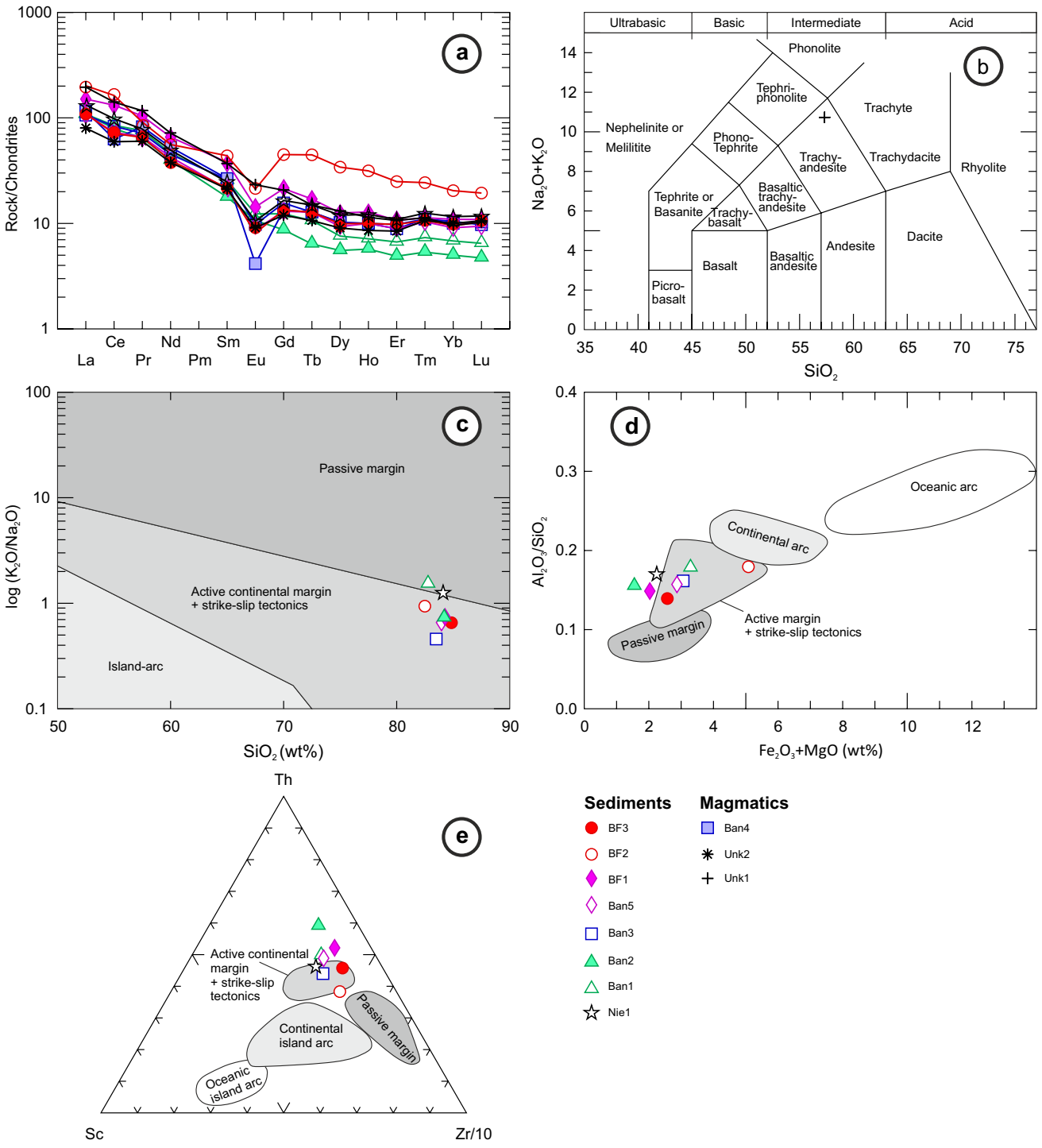

Fig. 11 Plots of geochemical data for samples from the Döhlen Basin. **a** Chondrite-normalized REE patterns (after Nakamura 1974) of all samples. The negative Eu anomaly of all samples except Unk1, Ban1 and Ban2 hints towards an erosion of crustal rocks (e.g., Gao and Wedepohl 1995). **b** TAS diagram for volcanic rocks after Le Maitre et al. (1989) demonstrating that sample Unk1 plots in the field of trachyandesite. **c** Log (K_2O/Na_2O) vs SiO_2 discrimination diagram after Roser and Korsch (1986) for all sediments showing that all samples point to an active continental margin regime. **d, e** Al_2O_3/SiO_2 vs Fe_2O_3+MgO discrimination diagram after Bhatia (1983) and Th-Sc-Zr/10 discrimination diagram after Bhatia and Crook (1986) for all sedimentary samples. All show an active continental setting. Diagrams are based on data given in Supplementary Data

Elbe Valley Slate Complexes), which partially underlie the Döhlen Basin shows a prominent Mesoproterozoic age gap, as they are mainly derived from the West African Craton (e.g., Linnemann et al. 2011, 2014). This gap is also present in all analyzed samples (Table 1, Supplementary Data). Hence, Mesoproterozoic ages are scarce, the obtained $_{\varepsilon}$Hf(t) values plotting into the field of Mesoproterozoic crust result from a magma mixing in Permian. Similar data published by Luthardt et al. (2018) also support our interpretation, indicating recycling of evolved crustal basement.

Provenance of sediments and basin development

Age data of detrital zircon provides age constraints for the source of Döhlen Basin sediments. The detrital zircon record of sample Nie1 of the Niederhäslich Formation (Fig. 8) shows several considerable source areas. Peaks at 305 and 330 Ma indicate a possible small input of material from the Meissen Volcanic Complex and the Meissen Massif (Nasdala et al. 1999; Hofmann et al. 2009; Hoffmann et al. 2013). Due to missing peaks at c. 325 Ma and 295 Ma, the Variscan Tharandt Caldera (Breitkreuz et al. 2009) and the 'Potschappel Wilsdruff Porphyrite' (Hoffmann et al. 2013; this paper) to the north of the Döhlen Basin area may be excluded as possible sources. Sample Nie1 does not support the suggested main input of Variscan volcanics (Reichel and Schauer 2006). However, it supports the, by Hoffmann and Schneider (2005), proposed extension of the Niederhäslich Formation through sediment input and the consequent covering of the surrounding Variscan volcanic complexes preventing an erosion of latter and therefore, no input of zircons. As the sample was taken at the top of the Niederhäslich Formation (see Fig. 4), we assume a maximum extent of the sediment cover. Therefore, no erosion of Variscan zircons occurred, as all proximal Variscan zircon sources were covered by the successions of the Niederhäslich Formation. On the other side, the major amounts of Cadomian ages are evidence for the input of Cadomian basement. Corresponding basement complexes within the surrounding Döhlen Basin area are the Erzgebirge and the Nossen-Wilsdruff Slate Complex (see Fig. 2) with zircon ages of c. 500–580 Ma (Tichomirowa 2001; Linnemann et al. 2007). Neumann (1961) also suggested the Elbe Valley Slate Complex as a source area for the basin fill. The U–Pb age of 365 ± 12 Ma for spot a56 of sample Nie1 (Supplementary Data) might be an evidence for a sediment input coming from W–SW, as this age overlaps in error with a chloritic gneiss of the Nossen-Wilsdruff Slate Complex, which was dated by Armstrong (2001) at 375 ± 3 Ma (Fig. 12a).

The detrital zircon record of sample Nie1 (upper Niederhäslich Formation) might also contain some clues concerning the tectono-sedimentary setting of the Döhlen Basin. The formation starts with a basal conglomerate (see Figs. 3, 4), suggesting increased relief energy. This might indicate a tectonic reactivation of the half-graben during the deposition of the underlying Döhlen Formation, leading to further subsidence. During this development, the Variscan volcanics of the surrounding regions of the Döhlen Basin were eroded and deposited as fine-grained sandstones of the Döhlen Formation. This led to a decreasing amount of detrital Variscan zircon ages in the sediments of the Niederhäslich Formation. This also led to a relative increase of detrital Cadomian ages. For the final stage of the development of the Niederhäslich Formation, our data allow to assume a flat relief gradient with an exposed Cadomian basement. Further, we assume that the deposition of the Niederhäslich Formation took place during a tectonic quiescence with minor volcanic activity.

The sediments of the Bannewitz Formation developed slightly different characteristics for the side depression of Hainsberg-Quohren, compared to the main depression of Döhlen and the side depression of Kohlsdorf-Pesterwitz (see Figs. 3, 4).

Samples Ban1 and Ban2 of the Volcanic Rock Fanglomerate Subformation of the main depression of Döhlen show an almost similar age distribution. Both feature peaks at c. 303–305 Ma (Fig. 8) which is strong evidence for the Meissen Volcanic Complex as a possible source area. Hoffmann et al. (2013) dated in ignimbrite of the Meissen Volcanic Complex at 303 ± 3 Ma. Furthermore, Ban1 and Ban2 inherited centimeter-sized clasts of flow-structured porphyrites similar to the 'Dobritz-Fluidalporphyr' of the Meissen Volcanic Complex (Naumann and v. Cotta 1845). These clasts are angular and imply a deposition by debris flows, hyperconcentrated flows or lahars over a distance of 30 km (Smith and Lowe 1991, Reichel and Schauer 2006). Besides, both samples contain ages at c. 320 Ma (Fig. 8) which hints to a deposition of sediments derived from the Tharandt Caldera (Breitkreuz et al. 2009). There are also well-rounded centimeter-sized clasts of rhyolites, implying a different transport process. Reichel and Schauer (2006) proposed a transport by channels of alluvial fans, which may have caused the roundness of the clasts. Debris flows entering the Döhlen Basin from the NW getting mixed with the alluvial fans coming from the W may have formed the volcanic rock fanglomerates of the Bannewitz Formation. Zircon ages of c. 295 Ma found in samples Ban1 and Ban2 point towards an erosion of the trachyandesite of the Unkersdorf Formation, which is dated at 293 ± 5 Ma (Hoffmann et al. 2013; this paper; Figs. 6, 12b). The obtained zircon Th/U ratios of samples Ban1 and Ban2 also indicate a felsic to intermediate source melt (Fig. 9), which corresponds with the felsic to intermediate volcanics of the surrounding basin area. Sample Ban1 shows a peak at c. 310 Ma (Fig. 8). Hoffmann et al. (2013) dated the Teplice Ignimbrite of the upper Teplice-Altenberg Volcanic Complex with 309 ± 5 Ma, which might

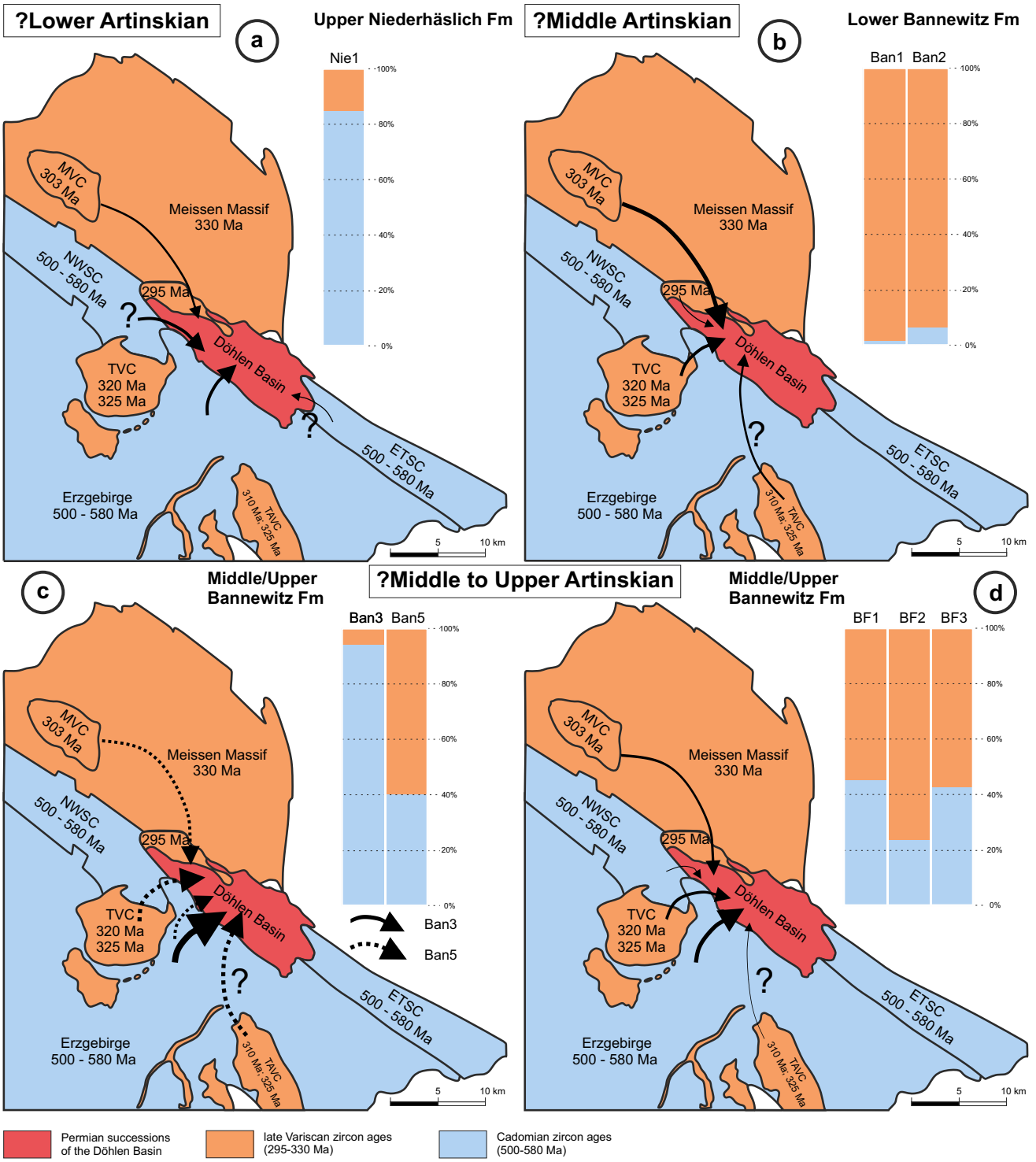

Fig. 12 Possible source areas of detrital zircons of the Döhlen Basin during the basin evolution and percentage of late Variscan to Cadomian zircon ages (map after Reichel and Schauer 2006); Bar charts are based on percentage distribution of obtained U/Pb ages. **a** Evolution of the late Niederhäslich Formation (sample Nie1). **b** Evolution of the early Bannewitz Formation (samples Ban1 and Ban2). **c, d** Evolution of the late Bannewitz Formation (samples Ban3, Ban5, BF1, BF2 and BF3). *NWSC* Nossen-Wilsdruff Slate Complex, *ETSC* Elbe Valley Slate Complex, *TVC* Tharandt Volcanic Complex, *TAVC* Teplice-Altenberg Volcanic Complex, *MVC* Meissen Volcanic Complex

be a possible source. After the tectonic quiescence during the deposition of the underlying Niederhäslich Formation, we suggest an active tectonic setting during the first phase of forming the Bannewitz Formation. Our data indicates that at least the initial formation stage was accompanied by major volcanic activity, which induced lahars or debris flows. The overwhelming amount of Variscan zircon ages of samples Ban1 and Ban2 (see Fig. 12b; Supplementary Data) are indicative for a strong magmatic activity during the time of deposition with a proposed SE directed sediment input from the Meissen Volcanic Complex as of matching U–Pb zircon ages (Hoffmann et al. 2013).

Depositional style changed after the high-volume input of debris flows into the Döhlen Basin during the Lower Bannewitz Formation. Samples Ban3 and Ban5 (see. Fig. 2) of the side depression of Hainsberg-Quohren show that compared to the above-discussed samples Ban1 and Ban2, the amount of Cadomian zircon ages has vastly increased, whereas Variscan ages decreased (Fig. 8). Nevertheless, the zircon age patterns for samples Ban3 and Ban5 differ strongly. Sample Ban3 from the gneiss rhyolite conglomerates contains big clasts of gneiss, The Erzgebirge in the S to SW of the Döhlen Basin features mainly Variscan gneisses containing Cadomian U–Pb zircon ages (e.g., Tichomirowa et al. 2001), which fits well with the obtained peak of Cadomian U–Pb ages in the samples Ban3 and Ban5. Therefore, the Erzgebirge is interpreted as the main source area for these sediments (Fig. 12d). There are no Devonian ages in these sediments, which would be typical for the Nossen-Wilsdruff Slate Complex and therefore can be neglected as a possible source. The small amount of Variscan ages is interpreted to be derived from reworked fanglomeratic material (for comparisons see age patterns for samples Ban1 and Ban2, Fig. 8). The Th/U ratios indicate felsic melts (see Fig. 9) which goes well along the Th/U ratios obtained by Hoffmann et al. (2013) for the big volcanic complexes surrounding the Döhlen Basin.

The environmental conditions were dominated by large alluvial fans coming out of the Erzgebirge area in the S and SW of the Döhlen Basin. The increasing amount of Variscan ages from sample Ban3 to sample Ban5 (see Fig. 7) might indicate that the Variscan cover of the Tharandt Caldera in the SW of the Döhlen Basin might as well have been a part of the drainage basin during Middle to Upper Artinskian times. The peak at 320 Ma fits well with the reported age by Breitkreuz et al. (2009) and references therein. Besides, the Th/U ratio and the REE pattern for sample Ban5 point to a felsic provenance (Figs. 9, 11a) in an active continental margin setting (Fig. 11c–e), which might also suggest the Tharandt Caldera to be an additional source area aside from the Erzgebirge gneiss. The age peak at 310 Ma (Fig. 8) possibly corresponds with the age for the Teplice-Altenberg Caldera (Fig. 2) given by Hoffmann et al. (2013). Transport distances from this Caldera to the Döhlen Basin are quite long, but now-eroded caldera outflow deposits might have been reworked and transported into the Döhlen Basin. Reichel and Schauer (2006) discussed alluvial plains as a depositional environment for the upper part of the Bannewitz Formation. In contrast to this consideration, sample Ban3 contains only a small amount of Variscan ages, whereas sample Ban5 shows considerable amounts of Variscan and Cadomian age groups. It might be that these two samples show the actual change of the depositional environment from an alluvial fan to an alluvial plain dominated system. Another possibility is an interfingering of several alluvial fans eroding Variscan volcanic and Cadomian basement material. The absence of c. 303 Ma old zircon ages is evidence of no subsequent reworking of the fanglomerates, whereas the Lower Bannewitz Formation (samples Ban1 and Ban2) shows almost no other ages besides the 303 Ma age peak (Fig. 8).

In the southwestern part of the Döhlen Basin, the amount of Cadomian ages did not increase. Samples BF1, BF2 (equivalents of the pyroclastic successions of Gittersee) and BF3 (gneiss rhyolite conglomerate) feature a slightly larger amount of Variscan (c. 60–80%) than Cadomian ages (c. 20–40%). Variscan peaks at c. 303 Ma and 320 Ma point to the Meissen Volcanic Complex and the Tharandt Caldera as possible source areas (Breitkreuz et al. 2009; Hoffmann et al. 2013, Figs. 6, 12d). The observed rhyolitic and flow-foliated rhyolitic clasts are also indicative for both considered source areas. Clasts of gneiss are evidence for the Variscan Erzgebirge Block as a third source area as well as the relatively large amount of Cadomian U–Pb ages (Tichomirowa et al. 2001, Fig. 8). Furthermore, the majority of Th/U ratios ranging from 0.1 to 1.0 pointing to a felsic provenance of the investigated samples (Figs. 9, 10a). The occurrence of Devonian U–Pb ages observed in the samples BF1, BF2 and BF3 may indicate a minor input of sediments of the Nossen-Wilsdruff Slate Complex (Armstrong 2001). A reworking of the underlying fanglomerates and a contemporaneous interfingering with deposits derived from the Erzgebirge gneiss might explain the occurrence Variscan and Cadomian zircon U–Pb ages in these samples (Fig. 8).

The exact locations of the eruption centers that created the analyzed tuff of Unkersdorf and the Wachtelberg ignimbritic tuff (samples Unk2 and Ban4) are still under discussion (e.g., Beck 1892; Hoffmann 2000; Reichel 1966; Reichel and Schauer 2006). The presented U–Pb ages of both samples might help to determine the vent locations. In our interpretation, they show a change of the volcanic activity during the evolution of the Döhlen Basin.

For sample Unk2 (Unkersdorf Tuff Subformation, see Fig. 3), Reichel and Schauer (2006) proposed the Meissen Volcanic Complex as a possible location, because of contained monzonitic and flow-foliated rhyolitic clasts within

the tuff. Hoffmann (2000) described andesitic, porphyritic and rhyolitic clasts, too. But the Meissen Volcanic Complex has an age of c. 303 Ma and also yields zircon ages of c. 330 Ma (Hoffmann et al. 2013). In contrast to that, the tuff sample Unk2 shows some zircon ages at c. 320 Ma (see Supplementary Data), which makes the Tharandt Volcanic Complex a more likely source area (see Fig. 2).

The second tuff sample (Ban4, Wachtelberg Ignimbrite) shows different zircon ages (see Supplementary Data). The diversity of zircon ages is much higher, which makes it difficult to determine a possible source area. Due to the diverse-inherited zircon ages of the Wachtelberg Ignimbrite (sample Ban4), it is not possible to determine the origin. Reichel and Schauer (2006) assumed the Tharandt Volcanic Complex as source area, which could not be verified by our data. The Wachtelberg Ignimbrite shows a very young depositional age of 286 ± 4 Ma, which does fit neither to the Tharandt nor to the Meissen Volcanic Complex. Ignimbrites of the Wurzen Complex were dated at 287 ± 3 Ma and 289 ± 4 Ma, respectively (Wendt et al. 1995; Repstock et al. 2018) going well with the obtained age for the Wachtelberg Ignimbrite. However, Wurzen ignimbrites are characterized with the presence of two pyroxenes, which do not occur in the Wachtelberg Ignimbrite (Reichel and Schneider 2012). Despite, an unknown and already eroded volcanic complex is also conceivable.

Conclusions

1. Radiometric data of three magmatic samples are interpreted to reflect initial and final phases of the evolution of the Döhlen Basin. The Unkersdorf Tuff (Unk2, 294 ± 3 Ma) and a trachyandesite overlying the tuff (Unk1, 293 ± 5 Ma) point to an initial basin formation during Lower Sakmarian times. The Wachtelberg Ignimbrite (Ban4, 286 ± 4 Ma) indicates a final development phase in the Middle Artinskian to Lower Kungurian. Our data implies an 8–15 Ma long-lasting basin evolution during an intense phase of volcanism at the Asselian-Sakmarian boundary, which can be correlated with a change from a convergent plate regime to strike-slip dominated tectonics in Central Europe. Geochemical data is also evidence for strike-slip tectonics and therefore a resulting formation of strike-slip-induced basins.
2. The development of the upper Niederhäslich Formation is considered to be dominated by an input of basement material shown by a vast amount of Cadomian zircon ages detected in sandstone sample Nie1. This hints towards a phase of volcanic quiescence with exposed Cadomian basement.
3. The evolution of the Bannewitz Formation may be divided into two distinct phases: The first is presumably dominated by large laharic or debris flow sediment inputs, whereas the second phase reflects an alluvial fan to alluvial plain environment. Samples Ban1 and Ban2 (volcanic rock fanglomerates) feature almost only Variscan zircon ages with a well-defined peak at c. 303 Ma which is a strong evidence for the Meissen Volcanic Complex as a possible source area. In addition, ages at c. 320 Ma may indicate the Tharandt caldera as a second source. During the evolution of the Bannewitz Formation, a significant facies change occurred. Samples of the overlaying Fanglomerate Subformation (Ban3, Ban5) show a significant shift in zircon age distribution with an increasing amount of Cadomian ages. This implies a simultaneously filling of the Döhlen Basin with basement and Variscan volcanic material by vast alluvial fans/plains out of SW direction. Samples BF1, BF2 and BF3 from the basin margin show the relatively homogenous mixing of Cadomian and Variscan sources during the late stage of the basin development.

Acknowledgements The authors thank R Krause for helpful assist during the laboratory work. The constructive comments and suggestions by R Rößler, F Breitkreuz and A von Quadt greatly helped to improve the manuscript. In addition, the authors would like to thank Prof. Wolf-Christian Dullo for his editorial work and help.

References

Ahrendt H, Clauer N, Hunziker J, Weber K (1983) Migration of folding and metamorphism in the Rheinische Schiefergebirge deduced from K-Ar and Rb-Sr age determinations. In: Martin H, Eder F (eds) Intracontinental fold belts. Springer, Berlin, Heidelberg, New York, pp 323–338

Alexosky W, Leonhardt D (1994) Geologische Übersichtskarte des Freistaates Sachsen 1:400.000. Karte ohne quartäre Bildungen. Sächsisches Landesamt für Umwelt und Geologie. Bereich Boden und Geologie, Dresden

Armstrong RA (2001) SHRIMP U–Pb zircon dating of the chlorite gneiss near Grumbach, west Dresden. Report A01-350b, Australian National University Canberra, p 4

Arthaud F, Matte P (1977) Late Paleozoic strike-slip faulting in southern Europe and northern Africa: results of a right-lateral shear zone between the Appalachians and the Urals. Geol Soc Am Bull 88:1305–1320

Awdankiewicz M, Breitkreuz C, Ehling B (2004) Emplacement textures in Late Palaeozoic andesite sills of the Flechtingen-Roßlau Block, north of Magdeburg (Germany). In: Breitkreuz C, Petford N (eds) Physical geology of high-level magmatic systems, vol 234. Geological Society, Special Publications, London, pp 51–66

Bayer U et al (2002) The southern margin of the East European Craton: new results from seismic sounding and potential fields between the North Sea and Poland. Tectonophysics 360:301–314. https://doi.org/10.1016/S0040-1951(02)00359-1

Beck R (1892) Sektion Kreischa-Hänichen. - Erläuterungen zur Geologischen Spezialkarte des Königreiches Sachsen, Nr. 82, Blatt Kreischa. K. Finanz-Ministerium, Leipzig, p 108

Benek R (1980) Geologisch-strukturelle Untersuchungen im Tharandter Vulkanitkomplex (Südteil der DDR). Z deutsh Geol Wiss 8:627–643

Benek R, Kramer W, McCann T, Scheck M, Negendank JFW, Korich D, Huebscher HD, Bayer U (1996) Permo-Carboniferous magmatism of the Northeast German Basin. Tectonophysics 266:379–404

Bhatia MR (1983) Plate tectonics and geochemical composition of sandstones. J Geol 91(6):611–627

Bhatia MR, Crook KAW (1986) Trace element characteristics of graywackes and tectonic setting discrimination of sedimentary basins. Contrib Mineral Petrol 92:181–193

Białek D, Kryza R, Oberc-Dziedzic T, Pin C (2014) Cambrian Zawidów granodiorites in the Cadomian Lusatian Massif (Central European Variscides): what do the SHRIMP zirconages mean? J Geosci 59:313–326

Borkowska M, Hameurt J, Vidal P (1980) Origin and age of Izera gneisses and Rumburk granites in the Western Sudetes. Acta Geol Pol 30:121–145

Bouvier A, Vervoort JD, Patchett PJ (2008) The Lu–Hf and Sm–Nd isotopic composition of CHUR: constraints from unequilibrated chondrites and implications for the bulk composition of terrestrial planets. Earth Planet Sci Lett 273:48–57. https://doi.org/10.1016/j.epsl.2008.06.010

Breitkreuz C, Kennedy A (1999) Magmatic flare-up at the Carboniferous/Permian boundary in the NE German Basin revealed by SHRIMP zircon ages. Tectonophysics 302:307–326. https://doi.org/10.1016/S0040-1951(98)00293-5

Breitkreuz C et al (2007) Far Eastern Avalonia: its chronostratigraphic structure revealed by SHRIMP zircon ages from Upper Carboniferous to Lower Permian volcanic rocks (drill cores from Germany, Poland, and Denmark). Geol Soc Am Spec Pap 423:173–190

Breitkreuz C, Renno AD, Schneider JW, Stanek K (2009) Late Paleozoic volcano sedimentary evolution of the Elbe Zone and the eastern Erzgebirge. Exkursionsf Veröff Deutsch Ges Geowiss 241:219–230

Chauvel C, Lewin E, Carpentier M, Arndt NT, Marini J-C (2007) Role of recycled oceanic basalt and sediment in generating the Hf–Nd mantle array. Nat Geosci 1:64. https://doi.org/10.1038/ngeo.2007.51

Fisher RV, Schmincke HU (1984) Pyroclastic rocks. Springer, Berlin

Förster H, Romer RL (2010) Carboniferous magmatism. In: Linnemann U, Romer R (eds) Pre-Mesozoic Geology of Saxo-Thuringia: from the Cadomian Active Margin to the Variscan Orogen. Schweizerbart, Stuttgart, pp 287–308

Franke W (2000) The mid-European segment of the Variscides: tectonometamorphic units, terrane boundaries and plate tectonic evolution. In: Franke W, Haak V, Oncken O, Tanner D (eds) Orogenic processes—quantification and Modelling in the Variscan Belt of Central Europe, vol 179. Geological Society, Special Publications, London, pp 35–61

Franke W, Żelaźniewicz A (2002) Structure and evolution of the Bohemian Arc. In: Winchester JA, Pharaoh TC, Verniers J (eds) Palaeozoic amalgamation of central Europe, vol 201. Geological Society, Special Publications, London, pp 279–293. https://doi.org/10.1144/GSL.SP.2002.201.01.13

Frei D, Gerdes A (2009) Precise and accurate in situ U–Pb dating of zircon with high sample throughput by automated LA-SF-ICP-MS. Chem Geol 261:261–270

Gao S, Wedepohl KH (1995) The negative Eu anomaly in Archean sedimentary rocks: Implications for decomposition, age and importance of their granitic sources. Earth Planet Sci Lett 133:81–94. https://doi.org/10.1016/0012-821X(95)00077-P

Gehmlich M (2003) Die Cadomiden und Varisziden des Saxothuringischen Terranes–Geochronologie magmatischer Ereignisse. Freib Forsch C500:1–129

Gehmlich M, Linnemann U, Tichomirowa M, Lützner H, Bombach K (1997) Die Bestimmung des Sedimentationsalters cadomischer Krustenfragmente im Saxothuringikum durch die Einzelzirkon–Evaporatisationsmethode. Terra Nostra 5:46–49

Geißler M, Breitkreuz C, Kiersnowski H (2008) Late Paleozoic volcanism in the central part of the Southern Permian Basin (NE Germany, W Poland): facies distribution and volcanotopographic hiati. Int J Earth Sci 97:973–989

Gerdes A, Zeh A (2006) Combined U–Pb and Hf isotope LA-(MC)-ICP-MS analyses of detrital zircons: comparison with SHRIMP and new constraints for the provenance and age of an Armorican metasediment in Central Germany. Earth Planet Sci Lett 249:47–61

Gerdes A, Zeh A (2009) Zircon formation versus zircon alteration: new insights from combined U–Pb and Lu–Hf in situ LA-ICPMS analyses, and consequences for the interpretation of Archean zircon from the Central Zone of the Limpopo Belt. Chem Geol 261:230–243

Gradstein FM, Ogg JG, Hilgen FJ (2012) On the geologic time scale. Newsl Stratigr 45:171–188

Hausse R (1892) Profile durch das Steinkohlenbecken des Plauen'schen Grundes (das Döhlener Becken) bei Dresden. K. Finanz-Ministerium, Leipzig, p 116

Heeremans M, Faleide J, Larsen BT (2004) Late Carboniferous Permian of NW Europe: an introduction to a new regional map. Geol Soc Lond Spec Publ 223:75–88

Hoffmann U (2000) Pyroklastite und Silicite im Rotliegend des Döhlen-Becken Stratigraphie, Genese und Paläontologie. Diploma thesis, TU BA Freiberg

Hoffmann U, Schneider JW (2005) Jungpaläozoikum der Döhlener Senke. In: Alexowsky W, Hoffmann U, Horna F, Kurze M, Schneider J, Tröger KA (eds) Geologische Karte des Freistaates Sachsen 1:25000, Erläuterungen zu Blatt 4947 Wilsdruff. Sächsisches Landesamt für Umwelt und Geologie (LfUG), Freiberg, pp 25–57

Hoffmann U, Breitkreuz C, Breiter K, Sergeev S, Stanek K, Tichomirowa M (2013) Carboniferous—Permian volcanic evolution in Central Europe—U/Pb ages of volcanic rocks in Saxony (Germany) and northern Bohemia (Czech Republic). Int J Earth Sci 102(1):73–99

Hofmann M, Linnemann U, Gerdes A, Ullrich B, Schauer M (2009) Timing of dextral strike-slip processes and basement exhumation in the Elbe Zone (Saxo-Thuringian Zone): the final pulse of the Variscan Orogeny in the Bohemian Massif constrained by LASF-ICP-MS U–Pb zircon data. Geol Soc Spec Publ 327:197–214

Hoskin PWO, Schaltegger U (2003) The composition of zircon and igneous and metamorphic petrogenesis. Rev Mineral Geochem 53:27–62. https://doi.org/10.2113/0530027

Jackson SE, Pearson NJ, Griffin WL, Belousova EA (2004) The application of laser ablation-inductively coupled plasma-mass spectrometry to in situ U-Pb zircon geochronology. Chem Geol 211:47–69

Katzung G (1995) Prä-Zechstein in Zntral- und Ostbrandenburg. Berl Geowiss Abh A 168:5–21

Knape H (1963a) Tektonischer Bau und Strukturgenese im nordwestlichen Vorland des Flechtinger Höhenzuges: Teil II: regionale Entwicklung und struktureller Bau. Geologie 12:637–673

Knape H (1963b) Tektonischer Bau und Strukturgenese im nordwestlichen Vorland des Flechtinger Höhenzuges; Teil I: stratigraphischer Überblick und Lagerungsverhältnisse. Geologie 1:509–536

Kossmat F (1927) Gliederung des varistischen Gebirgsbaues. G. A. Kaufmann's Buchhandlung, Dresden

Kroner U, Hahn T, Romer RL, Linnemann U (2007) The Variscan orogeny in the Saxo-Thuringian zone—Heterogenous overprint of Cadomian/Paleozoic Peri-Gondwana crust. In: Linnemann U, Nance RD, Kraft P, Zulauf G (eds) The evolution of the Rheic Ocean: From Avalonian-Cadomian active marginto Alleghenian-Variscan collision. Geological Society of America Special Paper 423, pp 153–172. https://doi.org/10.1130/2007.2423(06)

Kroner U, Romer RL, Linnemann U (2010) The Saxo-Thuringian Zone of the Variscan Orogen as part of Pangea. In: Linnemann U, Romer R (eds) Pre-Mesozoic geology of Saxo-Thuringia: from the Cadomian Active Margin to the Variscan Orogen. Schweizerbart, Stuttgart, pp 3–16

Kröner A, Hegner E, Hammer J, Haase G, Bielicki KH, Krauss M, Eidam J (1994) Geochronology and Nd-Sr systematics of Lusatian granitoids: significance for the evolution of the Variscan orogen in east-central Europe. Geol Rundsch 83:357–376

Kryza R, Pin C (1997) Cambrian/Ordovician magmatism in the Polish Sudetes: no evidence for subduction-related setting. EUG 9 Meeting, Strasbourg, p 144

Le Maitre RW, Bateman P, Dudek A, Keller J, Lameyre J, Le Bas MJ, Sabine PA, Schmid R, Sorensen H, Streckeisen A, Woolley AR, Zanettin B (1989) A classification of igneous rocks and glossary of terms. Blackwell, Oxford

Linnemann U (1994) Geologischer Bau und Strukturentwicklung der südlichen Elbe zone. Abhandlungen des Staatlichen Museums für Mineralogie Geologie zu Dresden 40:7–36

Linnemann U (2003a) Die Struktureinheiten des Saxothuringikums. In: Linnemann U (ed) Das Saxothuringikum, vol 48/49. Geologica Saxonica, Dresden, pp 19–28

Linnemann U (2003b) Sedimentation und geotektonischer Rahmen der Beckenentwicklung im Saxothuringikum (Neoproterozoikum—Unterkarbon). In: Linnemann U (ed) Das Saxothuringikum. Geologica Saxonica, vol 48/49. Dresden, pp 71–110

Linnemann U, Romer RL (2002) The Cadomian Orogeny in Saxo-Thuringia, Germany: geochemical and Nd–Sr–Pb isotopic characterisation of marginal basins with constraints to geotectonic setting and provenance. Tectonophysics 352:33–64

Linnemann U, Schauer M (1999) Die Entstehung der Elbezone vor dem Hintergrund der cadomischen und variszischen Geschichte des Saxothuringischen Terranes—Konsequenzen aus einer abgedeckten geologischen Karte. Zeitschrift für Geologische Wissenschaften 27(5/6):529–561

Linnemann U, Gerdes A, Drost K, Buschmann B (2007) The continuum between Cadomian orogenesis and opening of the Rheic Ocean: Constraints from LA-ICP-MS U-Pb zircon dating and analysis of plate-tectonic setting (Saxo-Thuringian zone, northeastern Bohemian Massif, Germany). In: Linnemann U, NanceRD, Kraft P, Zulauf G (eds) The evolution of the Rheic Ocean: from Avalonian-Cadomian active margin to Alleghenian-Variscan collision. Geological Society of America Special Paper 423, pp 61–96

Linnemann U, Romer RL et al (2008a) The Precambrian. In: McCann T (ed) The Geology of Central Europe. Geological Society, London, publications 21–102

Linnemann U, Pereira F, Jeffries TE, Drost K, Gerdes A (2008b) The Cadomian Orogeny and the opening of the Rheic Ocean: the diacrony of geotectonic processes constrained by LA-ICP-MS U–Pb zircon dating (Ossa-Morena and Saxo-Thuringian Zones, Iberian and Bohemian Massifs). Tectonophysics 461:21–43

Linnemann U, Ouzegane K, Drareni A, Hofmann M, Becker S, Gärtner A, Sagawe A (2011) Sands of West Gondwana: an archive of secular magmatism and plate interactions — A case study from the Cambro-Ordovician section of the Tassili Ouan Ahaggar (Algerian Sahara) using U-Pb–LA-ICP-MS detrital zircon ages. Lithos 123:188–203

Linnemann U, Gerdes A, Hofmann M, Marko L (2014) The Cadomian Orogen: Neoproterozoic to Early Cambrian crustal growth and orogenic zoning along the periphery of the West African Craton—Constraints from U–Pb zircon ages and Hf isotopes (Schwarzburg Antiform, Germany. Precambr Res 244:236–278

Lorenz V, Haneke J (2004) Relationship between diatremes, dykes, sills, laccoliths, intrusive-extrusive domes, lava flows, and tephra deposits with unconsolidated water-saturated sediments in the late Variscan intermontane Saar-Nahe Basin, SW Germany. Geol Soc Lond Spec Publ 234:75–124

Lorenz V, Nicholls IA (1984) Plate and intraplate processes of Hercynian Europe during the late Paleozoic. Tectonophysics 107:25–56

Ludwig KR (2001) User manual for Isoplot/ex rev. 2.49. Berkeley Geochronology Center Special Publications 1a, pp 1–56

Luthardt L, Hofmann M, Linnemann U, Gerdes A, Marko L, Rößler R (2018) A new U-Pb zircon age and a volcanogenic model for the early Permian Chemnitz Fossil Forest. Int J Earth Sci 107:2465–2489

Mattern F (1996) The Elbe zone at Dresden-a Late Paleozoic pull-apart intruded shear zone. Z deutsch Geol Ges 147:57–80

Mattern F (2001) Permo-Silesian movements between Baltica and Western Europe: tectonics and "basin families". Terra Nova 13:368–375

Nakamura N (1974) Determination of REE, BA, FE, Mg, Na and K in carbonaceous and ordinary chrondrites. Geochim Cosmochim Acta 38:757–775

Nance RD, Murphy JB (1996) Basement isotopic signatures and Neoproterozoic paleogeography of Avalonian-Cadomian and related terranes in the Circum-North Atlantic. In: Nance RD, Thompson MD (eds) Avalonian and related peri-Gondwanan terranes of the Circum-North Atlantic. Geological Society of America Special Paper 304, pp 333–346. https://doi.org/10.1130/0-8137-2304-3.333

Nance RD, Murphy JB, Keppie JD (2002) A Cordilleran model for the evolution of Avalonia. Tectonophysics 352:11–31

Nance RD, Murphy JB, Strachan RA, Keppie JD, Gutiérrez-Alonso G, Fernández-Suárez J, Quesada C, Linnemann U, D'lemos R, Pisarevsky SA (2008) Neoproterozoic-early Palaeozoic tectonostratigraphy and palaeogeography of the peri-Gondwanan terranes: Amazonian v. West African connections. In: Ennih N, Liégeois J-P (eds) The boundaries of the West African craton, vol 297. Geological Society, Special Publications, London, pp 345–383

Nance RD, Gutierrez-Alonso G, Keppie JD, Linnemann U, Murphy JB, Quesada C, Strachan RA, Woodcock NH (2012) A brief history of the Rheic Ocean. Geosci Front 3:125–135

Nasdala L, Wenzel Th, Pidgeon RT, Kronz A (1999) Internal structures and dating of complex zircons from Meissen Massif monzonites, Saxony. Chem Geol 156:331–341

Naumann CF, Cotta VB (1845) Geognostische Beschreibung des Königreiches Sachsen, Erläuterungen zu Section X. Geognostische Skizze der Umgebung von Dresden und Meißen. Arnoldische Buchhandlung, Dresden

Neumann E (1961) Die Geröllführung der Konglomerathorizonte des Rotliegenden im SE-Teil des Döhlener Beckens. Diploma thesis, TU BA Freiberg

Neumann ER, Wilson M, Heeremans M, Spencer EA, Obst K, Timmerman MJ, Kirstein L (2004) Carboniferous-Permian rifting and magmatism in southern Scandinavia, the North Sea and northern Germany: a review. Geol Soc Spec Publ 223:11–40

Oberc-Dziedzic T, Kryza R, Pin C, Mochnacka K, Larionov A (2009) The Orthogneiss and Schist Complex of the Karkonosze–Izera Massif (Sudetes, SW Poland): U–Pb SHRIMP zircon ages, Nd-isotope systematics and protoliths. Geol Sudet 41:3–24

Obst K, Katzung G, Hammer J (1999) Dating of the Late Autunian basic magmatism in the Thuringian Forest. N Jb Geol Palaeont Mh 1999:1–10

Pietzsch K (1956) Die Elbtalzone. Berichte der Geologischen Gesellschaft der Deutschen Demokratischen Republik 1:117–135

Pietzsch K (1963) Geologie von Sachsen. VEB Deutscher Verlag der Geowissenschaften, Berlin

Pin C, Marini F (1993) Early Ordovician continental break up in Variscan Europe: Nd–Sr isotope and trace element evidence from bimodal igneous associations of the southern Massif Central. France Lithos 29:177–196

Pin C, Kryza R, Oberc-Dziedzic T, Mazur S, Turniak K, Waldhauserová J (2007) The diversity and geodynamic significance of Late Cambrian (ca. 500 Ma) felsic anorogenic magmatism in the northern part of the Bohemian Massif: a review based on Sm-Nd isotope and geochemical data. In: Linnemann U, Nance RD, Kraft P, Zulauf G (eds) The evolution of the Rheic Ocean: from avalonian-cadomian active margin to alleghenian-variscan collision. Geological Society of America Special Paper 423, pp 209–229

Reichel W (1966) Stratigraphie, Paläogeographie und Tektonik des Döhlener Beckens bei Dresden. Dissertation, TU BA Freiberg

Reichel W (1970) Stratigraphie, Paläogeographie und Tektonik des Döhlener Beckens bei Dresden. Abhandlungen des Staatlichen Museum für Mineralogie Geologie zu Dresden 17:1–133

Reichel W (1985) Schichtstörungen im unterprmischen Döhlener Becken bei Dresden. Ein Beitrag zur lithofaziellen und tektonischen Entwicklung eines intramontanen vulkanotektonischen Beckens. Hallesches Jahrbuch für Geowissenschaften 10:21–34

Reichel W, Lange JM (2007) Cherts (Hornsteine) aus dem Döhlener Becken bei Dresden. Geologica Saxonica 52/53:117–128

Reichel W, Schauer M (2006) Das Döhlener Becken bei Dresden / Geologie und Bergbau. Sächsisches Landesamt für Umwelt und Geologie (LfUG), Dresden

Reichel W, Schneider JW (2012) Rotliegend im Döhlen-Becken. Schriftenreihe der Deutschen Gesellschaft für Geowissenschaften 61:589–625

Repstock A, Breitkreuz C, Lapp M, Schulz B (2018) Voluminous and crystal-rich igneous rocks of the Permian Wurzen volcanic system, northern Saxony, Germany: physical volcanology and geochemical characterization. Int J Earth Sci 107:1485–1513. https://doi.org/10.1007/s00531-017-1554-x

Robardet M (2002) Alternative approach to the Variscan Belt in southwestern Europe: preorogenic paleobiogeographical constraints. In: Martinez Catalán MR, Hatcher RD Jr, Arenas R, García FD (eds) Variscan-Appalachian dynamics: The building of the late Paleozoic basement. Geological Society of America Special Paper 364, pp 1–15. https://doi.org/10.1130/0-8137-2364-7.1

Röllig G (1976) Zur Petrogenese und Vulkanotektonik der Pyroxenquarzporphyre (Ignimbrite) des Nordwestsächsischen Vulkanitkomplexes. Jb Geol 5:176–268

Romer RL, Linnemann U, Gehmlich M (2003) Geochronologische und isotopengeochemische Randbedingungen für die cadomische und variszische Orogenese im Saxothuringikum. In: Linnemann U (ed) Saxothuringikum Das, vol 48/49. Geologica Saxonica, Dresden, pp 19–28

Roser BP, Korsch RJ (1986) Determination of Tectonic Setting of Sandstone-mudstone Suites Using SiO2 Content and K2O/Na2O Ratio. J Geol 94(5):635–650

Rößler R, Barthel M (1998) Rotlignd taphocoenoses preservation favoured by rhyolithic explosive volcanism. Freib Forsch H C474:59–101

Rößler R, Kretzschmar R, Annacker V, Mehlhorn S, Merbitz M, Schneider J, Luthardt L (2009) Auf Schatzsuche in Chemnitz–Wissenschaftliche Grabungen'09 Veröffentlichungen des. Museums für Naturkunde Chemnitz 32:25–46

Sagawe A, Gärtner A, Linnemann U, Hofmann M, Gerdes A (2016) Exotic crustal components at the northern margin of the Bohemian Massif—implications from U–Th–Pb and Hf isotopes of zircon from the Saxonian Granulite Massif. Tectonophysics 681:234–249

Schmiedel T, Breitkreuz C, Görz I, Ehling B (2015) Geometry of laccolith margins: 2D and 3D models of the Late Paleozoic Halle Volcanic Complex (Germany). Int J Earth Sci 104:323–333

Schneider JW (1994) Environment, biotas and taphonomy of the Lower Permian lacustrine Niederhäslich limestone, Döhlen basin, Germany. Trans R Soc Edinburgh Earth Sci 84:453–464

Schneider JW, Gebhardt U (1992) Dasycladaceen und andere "marine" Algen in lakustrischen Kalken des Unter-Perm (Assel) im intramontanen Döhlen Becken (Elbe-Zone). Freib. Forsch H C 445:66–88

Schneider JW, Hoffmann U (2001) Jungpaläozoikum der Döhlener Senke. In: Alexowsky W, Schneider JW, Tröger KA, Wolf L (eds) Geologische Karte des Freistaates Sachsen 1: 25 000, Erläuterungen zu Blatt 4948 Dresden. Sächsisches Landesamt für Umwelt und Geologie, Freiberg, pp 15–40

Schneider JW, Romer RL (2010) The Late Variscan Molasses (Late Carboniferous to Late Permian) of the Saxo-Thuringian Zone. In: Linnemann U, Romer RL (eds) Pre-Mesozoic Geology of Saxo-Thuringia. Schweizerbart, Stuttgart, pp 323–346

Schneider JW, Rössler R, Gaitzsch B (1995) Time lines of the Late Variscan volcanism—holostratigraphic synthesis. Zentralblatt für Geologie und Paläontologie Teil I 5(6):477–490

Schneider J, Rößler R, Fischer F (2012) Rotliegend des Chemnitz-Beckens (syn. Erzgebirge-Becken). In: Lützner H, Kowalczyk G (eds) Stratigraphie von Deutschland X. Rotliegend. Teil I: Innervariscische Becken, vol 61. Schriftenr. Dt. Ges. Geowiss, Hannover, pp 530–588

Sircombe KN (2004) AGEDISPLAY: an EXCEL workbook to evaluate and display univariate geochronological data using binned frequency histograms and probability density distributions. Comput Geosci 30(1):21–31

Slama J, Kosler J, Concon DJ, Crowley JL, Gerdes A, Hanchar JM, Horstwood MSA, Morris GA, Nasdala L, Norberg N, Schaltegger U, Schoene B, Tubrett MN, Whitehouse MJ (2008) Plesovice zircon—a new natural reference material for U–Pb and Hf isotopic microanalysis. Chem Geol 249:1–35

Smith G, Lowe DR (1991) Lahars: volcano – hydrologic events and deposition in the debris flow-hyperconcentrated flow continuum. In: Fisher R, Smith G (eds) Sedimentation in Volcanic Settings, vol 45. SEPM Specual Publication, Tulsa, OK, pp 60–70

Stacey J, Kramers J (1975) Approximation of terrestrial lead isotope evolution by a two-stage model. Earth Planet Sci Lett 26(2):207–221

Sterzel JT (1881) Über die Flora der unteren Schichten des Plauenschen Grundes. Z deutsh Geol Ges 33:339–347

Sterzel JT (1893) Die Flora des Rothliegenden im Plauenschen Grunde bei Dresden. Abhandlungen der Mathematisch-Physikalischen Classe Königlich Sächsischen Gesellschaft der Wissenschaften 19:1–172

Stille H (1949) Uralte Anlagen in der Tektonik Europas. Z deutsh Geol Ges 99:150–174

Tichomirowa M, Berger H-J, Koch EA, Belyatski BV, Götze J, Kempe U, Nasdala L, Schaltegger U (2001) Zircon ages of high-grade Gneisses in the eastern Erzgebirge (Central European Variscides)—constraints on origin of the rocks and Precambrian to Ordovician magmatic events in the Variscan foldbelt. Lithos 56:303–332

Tröger K-A, Behr H-J, Reichel W (1968) Die tektonisch-fazielle Entwicklung des Elbelineaments im Bereich der Elbtalzone. Freib Forsch H C241:71–85

Walther D et al (2016) The Late Carboniferous Schönfeld-Altenberg Depression on the NW margin of the Bohemian Massif (Germany/Czech Republic): volcano sedimentary and magmatic evolution. J Geosci 61:371–393

Wang X, Griffin WL, Chen J, Huang P, Li X (2011) U and Th contents and Th/U ratios of Zircon in felsic and mafic magmatic rocks: improved zircon-melt distribution coefficients. Acta Geol Sin 85:164–174

Wendt I, Höhndorf A, Wendt JI, Müller P, Wetzel K (1995) Radiometric dating of volcanic rocks in NW-Saxony by combined use of U–Pb and Sm-Nd zircon dating as well as Sm-Nd and Rb-Sr whole rock and mineral systematics. 11th meeting on geodynamics of eurpean Variscides, 2nd Symposium on Permocarboniferous igneous rocks. Terra Nostra Potsdam 7:147–148

Werneburg R, Schneider JW (2006) Amphibian biostratigraphy of the European Permo-Carboniferous. Geol Soc Lond Spec Publ 265(1):201–215

Ziegler P (1990) Geological Atlas of Western and Central Europe. Geological Society Publishing House, London